POSSIBLE STATIONARY POTENTIAL DISTRIBUTIONS OF A COLLISIONLESS TWO-EMITTER CS-DIODE

M. Troppmann

IPP 2/82 August 1969

INSTITUT FÜR PLASMAPHYSIK

GARCHING BEI MÜNCHEN

INSTITUT FÜR PLASMAPHYSIK

GARCHING BEI MÜNCHEN

POSSIBLE STATIONARY POTENTIAL DISTRIBUTIONS OF A COLLISIONLESS TWO-EMITTER CS-DIODE

M. Troppmann

IPP 2/82 August 1969

Die nachstehende Arbeit wurde im Rahmen des Vertrages zwischen dem Institut für Plasmaphysik GmbH und der Europäischen Atomgemeinschaft über die Zusammenarbeit auf dem Gebiete der Plasmaphysik durchgeführt.

IPP 2/82

M. Troppmann

Possible Stationary Potential Distributions of a Collisionless Two-Emitter Cs-Diode
(in English)
August 1969

Abstract

The POISSON equation together with boundary conditions suitable for a plasma diode with two equally heated emitter plates has been solved for stationary particle velocity distribution functions. The non-collision approximation is used and trapped particles are neglected.
Overlapping of the ranges of existence of the different types of potential shapes and consequently an ambiguity of the mathematical solutions of the problem is found. Except for these regions the non-monotonic potential shapes are uniquely determined by the boundary conditions in the case of ion rich emission of both end plates. A shape characterized by monotonic potential variation within both sheaths results in this case. On the other hand, for electron rich emission always two distinct shapes occur. One solution has an electron rich sheath in front of each emitter, the other one has a double sheath with its negative face nearest to the "negative" emitter at $-\xi_d$ and an electron sheath at the other plate.

A criterion of stability is not given in the framework of this paper. However, the necessary additional condition $F(y) \geq 0$ ($F(y) \equiv$ square of the normalized electric field strength) reduces the number of ambiguous (mathematical)solutions of the problem.

TABLE OF CONTENTS

LIST OF SYMBOLS

Symbol	Definition
d	half the distance between the two emitter plates
E	electric field strength, $E = - dV/dx$
E(x)	error function, $E(x) = \mathrm{erf}(x^{1/2}) = \frac{2}{\sqrt{\pi}} \int_0^{x^{1/2}} \exp(- t^2)dt$
e	absolute magnitude of the electron charge
F(η)	square of the normalized electric field, $F(\eta) = (\eta')^2$
f(x,v)	velocity distribution function
G(η)	$G(\eta) = \exp(\eta)\left[1 - E(\eta)\right] + 2(\eta/\pi)^{1/2} - 1$
g	statistical weight
H(η)	$H(\eta) = \exp(\eta)\left[1 + E(\eta)\right] - 2(\eta/\pi)^{1/2} - 1$
h	PLANCK's constant
I	ionization potential
j	current density
k	BOLTZMANN's constant
L	emission DEBYE-length, $L = (kT/8\pi e^2 N_{-\rightarrow}(-\eta_d))^{1/2}$
m	particle mass
N	particle density
n	normalized particle density
$\vec{n}_-$	$\vec{n}_-(\xi) = \vec{N}_-(\xi)/\vec{N}_-(-\xi_d)$
$\overleftarrow{n}_-$	$\overleftarrow{n}_-(\xi) = \overleftarrow{N}_-(\xi)/\overleftarrow{N}_-(+\xi_d)$
$\vec{n}_+$	$\vec{n}_+(\xi) = \vec{N}_+(\xi)/\vec{N}_+(-\xi_d)$
$\overleftarrow{n}_+$	$\overleftarrow{n}_+(\xi) = \overleftarrow{N}_+(\xi)/\overleftarrow{N}_+(+\xi_d)$
P	ionization coefficient
T	temperature of the emitter
V	potential
v	velocity of the charge carrier
x	distance variable
z	$z = \eta + \eta_d \ll 1$
α	$\alpha = \vec{N}_+(-\xi_d)/\vec{N}_-(-\xi_d)$
ß	$ß = \overleftarrow{N}_-(+\xi_d)/\vec{N}_-(-\xi_d)$
ν	$\nu = \overleftarrow{N}_+(+\xi_d)/\vec{N}_-(-\xi_d)$
ε	total energy of a particle
η	normalized potential, $\eta = eV/kT$
ν	evaporation rate
ξ	normalized distance variable, $\xi = x/L$
ρ	space charge density
Φ	work function (measured in volts)

Superscript

*	value at the emitter II (see appendix A)

Subscript

1,I	emitter at $-\xi_d$
2,II	emitter at $+\xi_d$
α	value at the emitter
e	value at the extremum
-	electron
+	ion
o	neutral particle
→	particle moves from emitter I to emitter II
←	particle moves from emitter II to emitter I

1. INTRODUCTION

The work on the collisionless description of a low-pressure thermionic converter originates from AUER and HURWITZ /1/ who investigated the various possible dc states of such a device. This work was later extended by McINTYRE /2/.

EICHENBAUM and HERNQVIST /3/ studied the electrostatic potential distributions of a "two-emitter diode" with no net current flowing through the device. They demonstrated the possibility of ambiguous solutions of POISSON's equation under certain conditions. Later on, applying AUER's method to the collisionless emitter sheaths of a Q-machine, RYNN /4/supposed nonmonotonic potential distributions to exist there. Experimentally, no evidence supporting this assumption has been found up to now. More recently two papers were published by SESTERO and ZANNETTI /5/ and HU and ZIERING /6/ respectively, dealing with collisionless plasma sheaths. The former authors considered different temperatures of the electrodes of a two-emitter device, but postulated a priori a monotonic change in the electric potential of the emitter sheath. The most important result was that even a small difference in temperatures of both emitter plates changes the picture drastically. HU and ZIERING presented a thorough analysis of a plasma sheath near an electrode including also microscopic boundary conditions, e.g. absorption, neutralization, and reflection, both diffusely and specularly, of the charge carriers.

Up to now only one aspect of the behaviour of the two-emitter diode -- the influence of a temperature difference between both plates -- has been discussed and even this in a nonrigid way. Other aspects, e.g. the ambiguity of solutions of POISSON's equation are only mentioned. Are these "static" solutions only of academic interest, or do they actually exist in a real diode? This question arises and has not found an answer up to now.

Therefore, our principle interest is to give a detailed analysis of the solutions of POISSON's equation restricted to the case of equal temperatures. We confine ourselves to this special case for two reasons: Firstly, this assumption simplifies the calculations in a high degree without limiting our interest in the ambiguity of the solutions. Secondly, the most interesting application of the present results is the Q-machine, which is usually operated with both plates at equal temperatures.

In chapter 2 all the assumptions used for discussing this problem are presented. A general procedure for obtaining the solutions of POISSON's equation is given in chapter 3. Then we shall deal with the monotonic potential shape discussing its boundaries in parameter space (chapter 4). Nonmonotonic potential distributions are described in chapter 5. The complexity of solutions in the case of electron rich emission of both emitter plates will be demonstrated. In chapter 6 the ambiguity of the various potential shapes found to the same boundary conditions will be considered.

These results have been obtained neglecting certain features of the problem, e.g. the effect of trapped particles. Possible consequences are discussed.

2. ASSUMPTIONS

We are dealing only with static potential distributions, i.e. we assume

$$\partial_t = 0.$$

The model of the one-dimensional low-pressure diode consists of two infinitely extended identical planar electrodes facing each other (diameter of the plates $\gg$ distance apart) (fig. 1) and heated to identical temperatures ($T_I = T_{II}$). The work function of both plates is assumed to be equal and the potential across their surfaces to be uniform. The mean free paths for encounters between the charge carriers are large compared with the DEBYE-length and with the diode spacing. Therefore, the electric field in the diode space is determined by POISSON's equation in its simplest form (in Gaussian units)

$$d^2V(x)/dx^2 = 4\pi e\left\{\vec{N}(x) + \overleftarrow{N}_-(x) - \vec{N}_+(x) - \overleftarrow{N}_+(x)\right\} \quad (1)$$

where the N's denote the various particle densities contributing to the space charge density. The arrows specify the possible directions of the velocity of the particles with respect to the x-coordinate.

The velocity distribution functions are described by the VLASOV equations for ions and electrons respectively

$$v\partial_x f_\pm \mp \frac{e}{m_\pm} E\,\partial_v f_\pm = 0 . \quad (2)$$

The electric field is given by $E = -dV/dx$
having only a component in the x-direction.

If elastic and inelastic collisions of short range are neglected, each charged particle interacts only with the COULOMB field of all the other ones. By using the method of characteristics we are able to integrate eq.(2). The solution can be expressed as

$$f_\pm = f_\pm(\varepsilon),$$

where

$$\varepsilon = \frac{1}{2} m_\pm v^2 \mp eV(x)$$

is the total energy of the particle which remains constant in the absence of collisions. We further assume that both electrons and ions issue with a Maxwellian velocity distribution corresponding to the plate temperature. The total flux density of the electrons is governed by the RICHARDSON-DUSHMAN equation

$$j_- = \frac{4\pi m_- ek^2}{h^3} T^2 \exp\left\{-\frac{e\Phi_-}{kT}\right\}$$

($e\Phi_-$ is the electron work function of the emitter /7/). The ion emission is given by the net current density of the neutrals and ions striking the emitter surface and their ionization probability P. The LANGMUIR-TAYLOR relation /8/ describes this process:

$$\nu_o/\nu_+ = \text{(neutral evaporation rate)/(ion evaporation rate)}$$
$$= \frac{g_o}{g_+} \exp\left\{-\frac{e(\Phi_+ - I)}{kT}\right\}.$$

The probability P is given by the relation

$$P = (1 + \nu_o/\nu_+)^{-1}.$$

$e\Phi_+$ is the effective work function of the process of ionization, being up to 0.5 eV higher than the electron work function $e\Phi_-$ /7/.

Neglecting collisions at all means to neglect the capture of charged particles about a potential extremum, keeping in mind that this is only a rough approach to reality. Even if the collision time is much larger than the transit time of a particle through the diode the probability of collisions is finite and therefore particles are existing which travel in closed orbits in phase space never touching one of the emitter surfaces. These trapped particles may alter the operating conditions of the diode substantially. If they are included into the model the spatially oscillatory solutions (to be discussed in a separate paper /9/) might vanish or at least decrease in amplitude. However, no reasonable assumption on the distribution function of the trapped particles has been established up to now /5, 10/.
The diode plates are assumed to be nonreflecting to incoming particles.

Processes of ionization and recombination may only occur at the hot endplates. This is true if the particle density is low enough to prevent volume processes.
The diode space, except two narrow sheaths near the electrodes, is occupied by a uniform plasma with vanishing space charge density

$$\rho_{\text{plasma boundary}} = 0. \tag{3}$$

Neglecting resistivity in the plasma body the electric field at the plasma boundary has to vanish

$$E_{\text{plasma boundary}} = 0. \tag{4}$$

According to the previously existing diode theory /2, 11/ the emission conditions of the diode are characterized by

$$\alpha \equiv \left(\frac{\vec{N}_+}{\vec{N}_-}\right)_{\text{neg.emitter}}$$

the ratio of densities of the charge carriers leaving the negative plate, and

$$\gamma \equiv \left(\frac{\overleftarrow{N}_+}{\overleftarrow{N}_-}\right)_{\text{pos.emitter}},$$

which describes the same quantity for the positive emitter. If α is larger than unity the state of emission of the diode is said to be ion rich. The emission is electron rich if $\alpha < 1$.

In the present paper the case $V_d > 0$ is considered only. Obviously, by interchanging the roles of both emitters and, therefore, of the parameters α and γ, the case $V_d < 0$ is described as well.

3. GENERAL DESCRIPTION

We shall give here a summary of the technique leading to the solutions of POISSON's equation. First-order ordinary differential equations are obtained which can only be solved numerically to get the potential as a function of the distance coordinate. If, however, one is interested in a survey of the shape of the potential distributions alone there is no need to perform this time-consuming numerical quadrature. The range of allowable parameters is obtained by simple calculations of $F'(\eta)$ and its first integral $F(\eta)$ as a function of η (a list of symbols used can be found on page iv). The main properties of the potential distribution can be seen from this procedure.

It turns out to be convenient to transform POISSON's equation (1) to reduced variables in order to eliminate as many parameters as possible from the equation,

$$\eta''(\xi) = \frac{1}{2}\left\{\vec{n}_-(\xi) + \beta\overleftarrow{n}_-(\xi) - \alpha\vec{n}_+(\xi) - \gamma\overleftarrow{n}_+(\xi)\right\},$$

where the prime denotes differentiation with respect to the argument.

The distribution functions of the particles as well as the particle densities are sectionally monotonic explicit functions of $V(x)$ and $\eta(\xi)$ respectively. Therefore, instead of the distance coordinate ξ we can use the normalized potential η as the variable:

$$F'(\eta) = \vec{n}_-(\eta) + \beta\overleftarrow{n}_-(\eta) - \alpha\vec{n}_+(\eta) - \gamma\overleftarrow{n}_+(\eta), \tag{5}$$

where we define

$$F(\eta) \equiv \eta'^2(\xi). \tag{6}$$

Since $T_I = T_{II}$
the RICHARDSON current densities $\vec{j}_-$ and $\overleftarrow{j}_-$ are equal which means

$$\beta \equiv \frac{\overleftarrow{j}_-(+\eta_d)}{\vec{j}_-(-\eta_d)} = 1.$$

For the ion current densities there does not exist such a simple expression. As shown in appendix B, the relation (eq.(B4)) holds

$$\gamma = \alpha \exp(-2\eta_d).$$

Integration of eq.(5) leads to an analytical expression of the electric field strength. (Both the space charge density and the electric field strength for the various shapes of potential distributions are shown in a general presentation in appendix A). Further integration yields the potential distribution, the formal solution of which is given by

$$\xi(\eta) = \int_{-\eta_d}^{\eta} (F(\eta) \mp 1)^{1/2} \, d\eta. \qquad (7)$$

Therefore, the problem of computing actual potential distributions is reduced to numerical quadrature. The externally controllable parameters are the dc potential difference $2\eta_d$, the distance $2\xi_d$ between the two emitter plates and the condition of ion rich or electron rich emission. Internal parameters include values at the potential extrema η_e, slope of the potential distribution near one of the emitters, which corresponds to $F(\mp \eta_d)$, and determination of the form of potential shapes possible under given conditions.

We classify the potential distributions as follows:

I. Uniform pontential in the diode plasma
   1. Potential shape of monotonic character, type A: One sheath being ion rich and the other one electron rich (fig. 2a).
   2. Nonmonotonic potential distributions
      Type B: both sheaths ion rich (fig. 2b).
      Type C: both sheaths electron rich (fig. 2c).
         a) The change in electric potential in both sheaths is monotonic (figs. 2(b1), 2(c1)).
         b) The potential shape has an extremum η_e in one of the emitter sheaths (figs. 2(b2-4), 2(c2-4)).

II. Spatially oscillatory solutions of POISSON's equation
    Potential distributions of this kind will be considered in a separate paper /9/.

Now, several models applying to the types of potential shapes mentioned above can be developed and their compatibility with the space charge equation and its first integral, the electric field equation be studied. The conditions defining the transition from sheath to the body of the plasma are equations (3) and (4).

The internal parameters are to be determined such that the integral in eq.(7) results in the given value of distance $2\xi_d$ of the two emitters. It should be noted that, except for the periodic types of potential distributions, the shape of the potential curve in the immediate vicinity of either electrode is rather insensitive to diode spacing as long as

$$\xi_d \gg 1.$$

Therefore, it is possible to assume infinite spacing in solving this problem numerically.

4. MONOTONIC POTENTIAL SHAPE (TYPE A)

At first we define the range of existence of type A in the parameter space α vs. η_d. Later on we have to distinguish between two cases according to the two possibilities of boundary conditions, i.e. vanishing electric field and vanishing space charge density respectively.

The criterion for a transition to a nonmonotonic potential distribution is a vanishing slope of the potential curve of shape A at one of the emitters.

4.1. Transition A to C (fig. 3a)

The potential distribution is described by

$$\eta_p \geq -\eta_d$$

and

$$\eta'(\eta)\Big|_{\eta=-\eta_d} \equiv (F(-\eta_d))^{1/2} = 0. \tag{8}$$

The space charge equation (A1) yields

$$\alpha = \tfrac{1}{2}\exp(2\eta_p)\left\{1 + \exp(2\eta_d) + E(\eta_p+\eta_d)\left[1 - \exp(2\eta_d)\right]\right\}. \tag{9}$$

Together with the condition on the electric field in the plasma volume, eq.(4), and the boundary condition, eq.(8), we arrive at an expression

$$g(\eta_p,\eta_d) \equiv G(\eta_p+\eta_d)\left[1 - \exp(-2\eta_d)\right] + 2\left[\exp(\eta_p-\eta_d) - \exp(-2\eta_d)\right] +$$

$$+\left[\exp(\eta_p-\eta_d) - \exp(2\eta_p)\right]\left\{1 + \exp(2\eta_d) + E(\eta_p+\eta_d)\left[1 - \exp(2\eta_d)\right]\right\} = 0. \tag{10}$$

To solve eq.(10) for given values of η_d, one solution can be specified immediately

$$\eta_p = -\eta_d.$$

As can be shown by numerical methods there exists another solution

$$\eta_p > -\eta_d$$

(fig. 4). The values α corresponding to a given set of values (η_p, η_d) may be calculated from eq.(9). Now the question arises:
Are both solutions of POISSON's equation

$$\eta_p = -\eta_d \text{ and } \eta_p > -\eta_d$$

realized? Due to the following argument the trivial solution must be excluded. Expanding the square of the electric field strength (eq.(A2))

$$F(\eta) = G(\eta+\eta_d)\left[1 - \exp(-2\eta_d)\right] + 2\left[\exp(\eta - \eta_d) - \exp(-2\eta_d)\right] +$$

$$+ 2\alpha\left[\exp(-\eta_d - \eta) - 1\right]$$

where the parameter α is calculated from eq.(9),

$$\alpha = \tfrac{1}{2}\left[1 + \exp(-2\eta_d)\right], \quad (\eta_p = -\eta_d),$$

for small values $z \equiv \eta + \eta_d \ll 1$ one gets

$$F(\eta) \approx \frac{4}{\sqrt{\pi}} z^{3/2}\left[\exp(-2\eta_d) - 1\right] + \ldots . \tag{11}$$

The term on the right-hand side of eq.(11) is negative. The square of the electric field strength, however, has to be positive definite. Hence the solution

$$\eta_p = -\eta_d$$

cannot be realized.

4.2. Transition A to B (fig. 3b)

In the transition from A to B the expressions

$$\eta'(\eta)\Big|_{\eta=+\eta_d} = 0, \tag{12}$$

$$\left.\begin{aligned} F(\eta;\alpha,\eta_d)\Big|_{\eta=\eta_p} &= 0 \\ \eta''(\eta;\alpha,\eta_d)\Big|_{\eta=\eta_p} &= 0 \end{aligned}\right\} \tag{13}$$

together with

$$\eta_p \leq +\eta_d,$$

must hold for the curve separating the two regions. The maximum slope $\eta'(\eta)\Big|_{\eta=-\eta_d}$ has to be calculated from the boundary condition (eq.(12)). Eliminating the parameter α from the two last expresssions (eqs.(13)) yields the equation

$$\begin{aligned} h(\eta_p,\eta_d) \equiv\ & \left[G(\eta_p+\eta_d) - G(2\eta_d)\right]\left[1-\exp(-2\eta_d)\right] + 2\left[\exp(\eta_p - \eta_d) - 1\right] \\ & + \left[\exp(\eta_p-\eta_d) - \exp(2(\eta_p-\eta_d))\right]\left\{1 + \exp(2\eta_d)\right. \\ & \left. + E(\eta_p+\eta_d)\left[1 - \exp(2\eta_d)\right]\right\} = 0. \end{aligned} \tag{14}$$

The relation

$$\eta_p = +\eta_d$$

satisfies eq.(14). It can be shown numerically that a further solution does not exist within the physically accessible range of parameters (α, η_d). The plausibility of this result can be seen in the following way. Both plates are emitting equal electron currents, whereas the ion production at the negative emitter E_I exceeds that of the positive emitter E_{II}; since the potential distribution directs most of the ion flux from the plasma to the negative plate. Furthermore, in the vicinity of plate I the ions stay always longer than at E_{II}; consequently, only near emitter I the space charge can be afforded to form a double sheath. Therefore, at the transition from A to B, a double sheath can never be formed in front of E_{II}.

4.3. Potential shape A: Vanishing space charge density near E_I

We have seen in the preceding consideration that a double sheath might be possible in front of emitter I. This forces to subdivide region A corresponding to the two possibilities:

1) vanishing electric field strength, $\eta' = 0$,
2) vanishing space charge, $\eta'' = 0$,

in the immediate vicinity of the negative emitter.

The first case has already been treated. Choosing vanishing space charge at the emitter $-\eta_d$ (fig. 3c) yields from eq.(A1)

$$\alpha = \tfrac{1}{2}\left[1 + \exp(-2\eta_d)\right].$$

To get the plasma potential η_p one has to solve

$$\begin{aligned} k(\eta_p,\eta_d) \equiv\ & \exp\left[2(\eta_p+\eta_d)\right]\left\{(1 + \exp(2\eta_d) + E(\eta_p+\eta_d)\left[1 - \exp(2\eta_d)\right]\right\} \\ & - 1 - \exp(2\eta_d) = 0. \end{aligned}$$

Except of the trivial solution $\eta_p = -\eta_d$, an additional solution $\eta_p > -\eta_d$ can be found

numerically. This solution is shown in fig. 5.

Again we have two solutions corresponding to the same external parameters (α, η_d). As in case 4.1. we arrive at

$$F(\eta) \approx F(-\eta_d) + \left\{ \frac{4}{\sqrt{\pi}} z^{3/2} \left[\exp(-2\eta_d) - 1\right]\right\} + \ldots .$$

The second term on the RHS is negative. Therefore, it is not possible that, at the same time, both space charge and electric field ($\hat{=} F(-\eta_d)$) in the vicinity of the emitter - η_d may vanish because this requires $\eta_p = -\eta_d$ to be possible as a solution.

Fig. 6 shows the range of existence for the monotonical potential shape A.

5. NONMONOTONIC POTENTIAL SHAPES

Investigating the models B and C of nonmonotonic potential distributions (fig. 2) we arrive at two expressions with the unknown quantities η_p and η_e. In general it is impossible to give an analytical solution. To obtain numerical solutions the procedure is as follows: The contour lines of the space charge and the electric field equation respectively are calculated and looked for common zeros.

5.1. Potential shape of type B

Firstly, we consider potential distributions of type B with only one potential maximum. Two cases may be distinguished

1) $\eta_p \geq +\eta_d$: The potential maximum is reached within the sheath in front of emitter ($-\eta_d$), (fig.2(b2)),
   emitter ($+\eta_d$), (fig. 2(b3)),
2) $\eta_p < +\eta_d$, (fig. 2(b4)).

It can be demonstrated that in the first case the space charge density does not depend on position and magnitude of the potential maximum (see eq.(A5)). Both opposite ion currents have to overcome the potential barrier. Their values, depending on the potential maximum, differ by the factor $\exp(-2\eta_d)$. The influx of fresh ions from the positive emitter, however, is reduced by just the same factor. Hence, no net ion current flows in the diode. Therefore, the shape must be symmetric about the potential maximum for values of η larger than $+\eta_d$.

Fig. 7 shows a plot of the second derivative of η as a function of η for the potential shape B for different values of η_d. Each of the curves rises to a maximum at its respective value of η_d, dips down and comes back again. As long as η'' does not reach zero in the range $\eta < +\eta_d$, the function η'' has only one zero (for some value $\eta > +\eta_d$). In this case, consequently, the potential distribution must have shape B (plasma potential equals to extremal potential). Therefore, all distributions with $\eta_p \neq \eta_e$ and $\eta_p > +\eta_d$ (figs. 2(b2,3)) are excluded.

In the second case to be discussed the plasma potential has to fulfil the condition $\eta_p < +\eta_d$, corresponding to more than one zero of the function $\eta''(\eta)$. One can see immediately from fig.7 that in a narrow range of values of η_d this potential shape (fig. 2(b4)) may be a solution of the space charge equation.

Summarizing, the solutions of type B are given by the shapes $\eta_p = \eta_e$ and $\eta_p \neq \eta_e$, $\eta_p < +\eta_d$. Fig. 8 presents a picture of η_e and η_p vs. η_d with α as a parameter.

5.2. Potential distributions of type C

We discuss the four models (fig. 2(c1-4)) analogous to those of type B. Contrary to the previous case (type B) both the functions of the space charge density and the electric field strength are different at the two sides of the potential minimum (eqs.(A7)...(A12)). This behaviour is caused by the charge carriers which contribute to the space charge in a different way for the cases B and C respectively. In the former case both ion currents of either direction have to overcome the potential barrier. As discussed in section 5.1., under these conditions the total ion current flowing through the diode is zero. On the other hand, in presence of case C the ions fall through the sheath potential near either emitter, whereas the electrons have to overcome the potential minimum. In this case terms with η_e do not cancel out.In this case, the equations cannot be solved analytically; results can only be obtained numerically. One has to calculate the contour lines of space charge and electric field equations for all three cases (fig. 2(c2-4)) separately and look for common zeros.

In the series of illustrations in fig. 9 we assume e.g. α to have the value 0.2. The point of intersection of the two contour lines results in a (mathematical) solution of POISSON's equation together with the specialized boundary conditions. As a result we can see: the potential distribution with $\eta_p < -\eta_d$ and a potential extremum inside the sheath near the positive emitter ($+\eta_d$) (fig. 2(c3), marked with II in fig. 9) has the only solution

$$\eta_p = \eta_e,$$

which means, that there exists a nonmonotonic potential shape with monotonic sheaths. Fig. 10 displays the potential minimum η_e as a function of the applied diode voltage η_d for different values of the parameter α.
For the other potential shapes I and III with $\eta_p \gtrless -\eta_p$ and a nonmonotonic sheath in front of the emitter ($-\eta_d$)(figs. 2(c2,c4)) the number of solutions depends on the value of the applied diode voltage.

Discussing the two cases separately, we see that there exists only the trivial solution $\eta_p = \eta_e$ for the potential distribution I (fig. 9) for values of η_d larger than 1.068. The difference in η_e of the contour lines F and F' respectively, is always negative if plasma potential η_p is fixed. At constant α with decreasing values of η_d the contour line of the space charge equation F' bulges and touches the electric field curve F. An additional solution with $\eta_p > \eta_e$ appears. Reducing η_d further the solution splits. A critical value $\eta_{d\,crit}$ is reached if one of the points of intersection coincides with the limiting line $\eta_p = -\eta_d$ ($\eta_{d\,crit} = 0.835\,607$). For values η_d smaller than this critical value $\eta_{d\,crit}$ there exist only two solutions which coincide at $\eta_d = 0$.

In case III there exists a solution only if η_d is larger than the above mentioned critical value $\eta_{d\,crit}$. For values of the parameter α lower than 0.4 the η_d-values are not limited, otherwise the upper limit of $\eta_d$depends on the combination of the values α and η_d. The limiting number pair (α, η_d) is given by the curve separating regions A from C (fig. 6). With large expense of calculations we computed the cut surface of the two four-parametric equations

$$F'(\eta_d;\eta_p,\eta_e,\alpha) = 0$$

and

$$F(\eta_d;\eta_p,\eta_e,\alpha) = 0.$$

Its projection into the planes η_d vs. η_p and η_d vs. η_e for the case of $\alpha = 0.2$ is shown in fig. 9a. The ambiguity of the solutions of POISSON's equation is obvious.
As a main result we can say: For the type C of the potential shapes always two solutions are existing, one with monotonic sheaths and the other one with a potential minimum in the sheath in front of the negative emitter ($-\eta_d$). In a small range of the external variables (α, η_d) two more solutions appear.
To achieve an impression of the variety of solutions of POISSON's equation with the assumption

of various boundary conditions fig. 11 shows a three-dimensional representation of the above mentioned cut surface. Again the complexity of type C of potential shapes (fig.11c) is clearly seen. For discussing the physical properties of this representation we make three cross-sections, one parallel to the axis of the parameter α (fig. 12) and other ones parallel to the axis of the diode voltage η_d (figs. 13 and 14).

6. SEQUENCE OF SOLUTIONS OF POISSON'S EQUATION AS A FUNCTION OF EXTERNAL VARIABLES

In a series of illustrations in figs. 12-14 we see some of the successive potential shapes (drawn schematically) appearing if α and η_d, respectively are varied.
In fig. 12 we assume η_d to have the value 1.2. Shapes of potential distributions are shown as a function of α. At first, if α decreases from very large values, only potential shapes of type B are found characterized by a uniform potential throughout most of the interelectrode volume and monotonic sheaths in front of each emitter plate (fig. 12(1)). The potential shape is nonambiguous until a point is reached where two solutions appear (fig. 12(2)), one of type B and one of type A, where the plasma potential is equal to the potential + η_d of the emitter at + ξ_d. One identifies this point as the transition point from potential shape A to B. As can be seen the potential distribution "B" may overlap the range of existence of solutions of type A by a small amount.

A further decrease in the parameter α will yield only monotonically increasing potential shapes (fig. 12(3-6)), case A, which persists until the slope of the potential curve in the immediate vicinity of the emitter I is reduced to zero (fig. 12(6)). As α is further decreased the potential curve will dip down in the region near the emitter I (fig.12(7)) exhibiting a shape which is one of the possible forms of type C. This distribution is characterized by a double sheath with the negative face nearest to the emitter at - ξ_d, whereas within the emitter-II region an electron sheath remains. Throughout the remainder of the diode volume there is a uniform potential η_p larger than the potential - η_d of the emitter I. In general, decreasing α implies decreasing plasma potential η_p. If η_p equals the negative emitter potential - η_d (fig. 12(9)) another critical point is reached in the vicinity of which several solutions of the space charge equation and its first integral exist and below which a shape is developed similar to the one described just above, but now with a plasma potential which is less than - η_d (fig. 12(10)).

For sake of simplicity we have omitted for the moment another branch of the curve denoted as "$\eta_p = \eta_e$" in fig. 12. For values α larger than the value corresponding to the lower limit of case A (fig. 12(6)), we find an additional potential distribution of type C, the sheaths of which are both monotonic (fig. 12(5)). It is the counterpart to the solution of shape "B" for α larger than the upper limit of shape "A".

It is worthwhile to point out the presence of <u>always two</u> shapes of type C, between the points (7) and (10) in fig. 12, one of the form just mentioned with two monotonic sheaths and one with a double sheath in front of the negative emitter. The plasma potential of the latter may be larger or lower than the negative emitter potential - η_d.
Figs. 13 and 14 show the shapes of potential distributions for varying diode voltage, where $\alpha = 0.65$ and $\alpha = 10$ respectively. The main features described are displayed again, i.e. overlapping ranges of existence of different types and therefore the ambiguity of the solutions of POISSON's equation in these regions.

7. DISCUSSION

It should be born in mind, that in the present state of discussion we cannot decide which of the possible potential distributions within the ambiguous regimes might really exist. A general decision must be reserved for future work. Another point is unsatisfactory up to now. We do not know any mechanism which produces a transition between the two solutions of type C for nonzero values of η_d. Only for zero diode voltage the two branches fall into each other (fig. 13).

We have to keep in mind furtheron that the solutions discussed here were obtained by looking "mechanically" for common zeros of the equations (3) and (4). To estimate, however, the physical significance of these results and to calculate explicitly the potential η as a function of the normalized distance ξ, it is absolutely necessary to know the character of the function $F(\eta)$ in the whole range of possible values of η. Solutions which are physically realizable are characterized by the condition

$$F(\eta) \geq 0 \qquad (15)$$

since $F(\eta)$ corresponds to the square of the normalized electric field strength. -- If we take into account this condition (15) some of the ambiguous solutions will vanish as shown in /9/.

8. SUMMARY

In this paper we calculated the solutions of POISSON's equation with boundary conditions suitable to a plasma diode. To simplify the effort of computation reasonable assumptions have been made. The most restricting one was to neglect the influence of the trapped particles. No reasonable form of their velocity distribution function has been established up to now. In addition, the spatially oscillatory potentials have been dropped from consideration.

The most interesting result is the overlapping of the ranges of existence of different types of potential shapes and therefore the occurrence of more than one solution of POISSON's equation compatible with the same boundary condition. No efforts have been made at present to decide which of them are really existing. Since the function $F(\eta)$corresponds to the square of the normalized electric field strength it has to be positive semidefinite for each value of η_d to yield actual potential distributions.

APPENDIX A

Reduced particle densities and electric field strengths (in the diode volume)

In the following a general presentation of reduced particle densities $n(\eta)$ and of the square of the electric field strength $F(\eta)$ in the diode volume will be given. Different temperatures of both end plates, T and T^* are assumed. Their corresponding surface potentials are η_1 and η_2 respectively. Six cases have to be distinguished (fig. 15). Using the abbreviations

$$E(\eta) \equiv \exp(\eta^{1/2}) = \frac{2}{\sqrt{\pi}} \int_0^{\eta^{1/2}} \exp(-t^2)dt,$$

$$G(\eta) \equiv \exp(\eta)\left[1 - E(\eta)\right] + 2(\eta/\pi)^{1/2} - 1,$$

$$H(\eta) \equiv \exp(\eta)\left[1 + E(\eta)\right] - 2(\eta/\pi)^{1/2} - 1,$$

$$= -G(\eta) + 2\exp(\eta) - 2,$$

one arrives at the following expressions for $n(\eta)$ and $F(\eta)$.

Case 1(a)

$$\vec{n}_-(\eta) = \exp(\eta-\eta_1)\left[1-E(\eta-\eta_1)\right],$$

$$\overleftarrow{n}_-(\eta) = \exp(\eta^*-\eta_2^*)\left[1+E(\eta^*-\eta_1^*)\right],$$

$$\overleftarrow{n}_+(\eta) = \exp(\eta_1-\eta)\left[1+E(\eta_2-\eta)\right],$$

$$\vec{n}_+(\eta) = \exp(\eta_2^*-\eta^*)\left[1-E(\eta_2^*-\eta^*)\right],$$

$$F(\eta) = F(\eta_1) + G(\eta-\eta_1) + \beta\delta\exp(\eta_1^*-\eta_2^*)H(\eta^*-\eta_1^*) +$$
$$+\alpha\exp(\eta_1-\eta_2)\left[H(\eta_2-\eta)-H(\eta_2-\eta_1)\right] +$$
$$+\gamma\delta\left[G(\eta_2^*-\eta^*)-G(\eta_2^*-\eta_1^*)\right].$$

Case 2(a)

$$\vec{n}_-(\eta) = \exp(\eta-\eta_1)\left[1+E(\eta-\eta_2)\right],$$

$$\overleftarrow{n}_-(\eta) = \exp(\eta^*-\eta_2^*)\left[1-E(\eta^*-\eta_2^*)\right],$$

$$\overleftarrow{n}_+(\eta) = \exp(\eta_1-\eta)\left[1-E(\eta_1-\eta)\right],$$

$$\vec{n}_+(\eta) = \exp(\eta_2^*-\eta^*)\left[1+E(\eta_1^*-\eta^*)\right],$$

$$F(\eta) = F(\eta_2) + \exp(\eta_2-\eta_1)H(\eta-\eta_2) + \beta\delta G(\eta^*-\eta_2^*) +$$
$$+\alpha\left[G(\eta_1-\eta)-G(\eta_1-\eta_2)\right] +$$
$$+\gamma\delta\exp(\eta_2^*-\eta_1^*)\left[H(\eta_1^*-\eta^*)-H(\eta_1^*-\eta_2^*)\right].$$

Case 1(b)

$$\vec{n}_-(\eta) = \exp(\eta-\eta_1)\left[1-E(\eta-\eta_1)\right],$$

$$\overleftarrow{n}_-(\eta) = \exp(\eta^*-\eta_2^*)\left[1+E(\eta^*-\eta_1^*)\right], \qquad \eta \le \eta_2$$
$$= \exp(\eta^*-\eta_2^*)\left[1-2E(\eta^*-\eta_2^*)+E(\eta^*-\eta_1^*)\right], \qquad \eta \ge \eta_2$$

$$\overleftarrow{n}_+(\eta) = \exp(\eta_1-\eta)\left[1+E(\eta_1-\eta)\right], \qquad \eta' \ge 0$$
$$= \exp(\eta_1-\eta)\left[1-E(\eta_1-\eta)\right], \qquad \eta' \le 0$$

$$\vec{n}_+(\eta) = \exp(\eta_2^*-\eta^*)\left[1+E(\eta_2^*-\eta^*)\right], \qquad \eta' \le 0$$
$$= \exp(\eta_2^*-\eta^*)\left[1-E(\eta_2^*-\eta^*)\right], \qquad \eta' \ge 0$$

$$F(\eta) = G(\eta-\eta_1) - G(\eta_2-\eta_1) + \beta\delta\left\{\exp(\eta_1^*-\eta_2^*)\left[G(\eta_2^*-\eta_1^*)-\right.\right.$$
$$\left.\left.-G(\eta^*-\eta_1^*)\right] + 2\left[\exp(\eta^*-\eta_2^*)-1-G(\eta_2^*-\eta_2^*)\right]\right\} +$$
$$+\alpha\exp(\eta_1-\eta_2)H(\eta_2-\eta) + \gamma\delta\exp(\eta_2^*-\eta_2^*)G(\eta_2^*-\eta^*),$$
$$\eta \le \eta_2, \ \eta' > 0$$

Case 2(b)

$$\vec{n}_-(\eta) = \exp(\eta-\eta_1)\left[1+E(\eta-\eta_2)\right], \qquad \eta' \le 0$$
$$= \exp(\eta-\eta_1)\left[1-E(\eta-\eta_2)\right], \qquad \eta' \ge 0$$

$$\overleftarrow{n}_-(\eta) = \exp(\eta^*-\eta_2^*)\left[1+E(\eta^*-\eta_2^*)\right], \qquad \eta' \ge 0$$
$$= \exp(\eta^*-\eta_2^*)\left[1-E(\eta^*-\eta_2^*)\right], \qquad \eta' \le 0$$

$$\overleftarrow{n}_+(\eta) = \exp(\eta_1-\eta)\left[1-E(\eta_1-\eta)\right],$$

$$\vec{n}_+(\eta) = \exp(\eta_2^*-\eta^*)\left[1-2E(\eta_2^*-\eta^*)+E(\eta_1^*-\eta^*)\right], \qquad \eta \le \eta_2$$
$$= \exp(\eta_2^*-\eta^*)\left[1+E(\eta_1^*-\eta^*)\right], \qquad \eta \ge \eta_2$$

$$F(\eta) = \exp(\eta_2-\eta_1)H(\eta-\eta_2) + \beta\delta\exp(\eta_2^*-\eta_2^*)G(\eta^*-\eta_2^*) +$$
$$+\alpha\left[G(\eta_1-\eta)-G(\eta_1-\eta_2)\right] + \gamma\delta\left\{\exp(\eta_2^*-\eta_1^*)\left[G(\eta_1^*-\eta_2^*)-\right.\right.$$
$$\left.\left.-G(\eta_1^*-\eta^*)\right] + 2\left[\exp(\eta_2^*-\eta^*)-1-G(\eta_2^*-\eta_2^*)\right]\right\},$$
$$\eta \ge \eta_2, \ \eta' < 0$$

$$= G(\eta-\eta_+) - G(\eta_c-\eta_+) + \beta\delta\{\exp(\eta_+^*-\eta_2^*)[G(\eta_c^*-\eta_+^*) - G(\eta^*-\eta_+^*)] + 2[G(\eta^*-\eta_2^*) - G(\eta_c^*-\eta_2^*)]\} +$$
$$+ \alpha\exp(\eta_+-\eta_c)\,\#(\eta_c-\eta) + \gamma\delta\exp(\eta_2^*-\eta_c^*)\,G(\eta_c^*-\eta^*),$$
$$\eta \geq \eta_2\,,\quad \eta' \geq 0$$

$$= G(\eta-\eta_+) - G(\eta_c-\eta_+) + \beta\delta\{\exp(\eta_+^*-\eta_2^*)[G(\eta_c^*-\eta_+^*) - G(\eta^*-\eta_+^*)] + 2[G(\eta^*-\eta_2^*) - G(\eta_c^*-\eta_2^*)]\} +$$
$$+ \alpha\exp(\eta_+-\eta_c)\,G(\eta_c-\eta) + \gamma\delta\exp(\eta_2^*-\eta_c^*)\,\#(\eta_c^*-\eta^*),$$
$$\eta \geq \eta_2\,,\quad \eta' \leq 0\,.$$

$$= \exp(\eta_c-\eta_+)\,\#(\eta-\eta_c) + \beta\delta\exp(\eta_c^*-\eta_2^*)\,G(\eta^*-\eta_c^*) +$$
$$+ \alpha[G(\eta_+-\eta) - G(\eta_+-\eta_c)] + \gamma\delta\{\exp(\eta_2^*-\eta_+^*)[G(\eta_+^*-\eta_c^*) - G(\eta_+^*-\eta^*)] + 2[G(\eta_2^*-\eta^*) - G(\eta_2^*-\eta_c^*)]\},$$
$$\eta \leq \eta_2\,,\quad \eta' \leq 0$$

$$= \exp(\eta_c-\eta_+)\,G(\eta-\eta_c) + \beta\delta\exp(\eta_c^*-\eta_2^*)\,\#(\eta^*-\eta_c^*) +$$
$$+ \alpha[G(\eta_+-\eta) - G(\eta_+-\eta_c)] + \gamma\delta\{\exp(\eta_2^*-\eta_+^*)[G(\eta_+^*-\eta_c^*) - G(\eta_+^*-\eta^*)] + 2[G(\eta_2^*-\eta^*) - G(\eta_2^*-\eta_c^*)]\},$$
$$\eta \leq \eta_2\,,\quad \eta' \geq 0\,.$$

Case 1(c)

$$\vec{n}_-(\eta) = \exp(\eta-\eta_+)[1 - 2E(\eta-\eta_+) + E(\eta-\eta_2)], \qquad \eta \geq \eta_+$$
$$= \exp(\eta-\eta_+)[1 + E(\eta-\eta_2)], \qquad \eta \leq \eta_+$$
$$\overleftarrow{n}_-(\eta) = \exp(\eta^*-\eta_2^*)[1 - E(\eta^*-\eta_2^*)],$$
$$\vec{n}_+(\eta) = \exp(\eta_+-\eta)[1 + E(\eta_c-\eta)], \qquad \eta' \geq 0$$
$$= \exp(\eta_+-\eta)[1 - E(\eta_c-\eta)], \qquad \eta' \leq 0$$
$$\overleftarrow{n}_+(\eta) = \exp(\eta_2^*-\eta^*)[1 + E(\eta_c^*-\eta^*)], \qquad \eta' \leq 0$$
$$= \exp(\eta_2^*-\eta^*)[1 - E(\eta_c^*-\eta^*)], \qquad \eta' \geq 0$$
$$F(\eta) = 2[G(\eta-\eta_+) - G(\eta_c-\eta_+)] + \exp(\eta_2-\eta_+)[G(\eta_c-\eta_2) - G(\eta-\eta_2)] + \beta\delta[G(\eta^*-\eta_2^*) - G(\eta_c^*-\eta_2^*)] + \alpha\exp(\eta_+-\eta_c) + \#(\eta_c-\eta) + \gamma\delta\exp(\eta_2^*-\eta_c^*)\,G(\eta_c^*-\eta^*),$$
$$\eta \geq \eta_+\,,\quad \eta' \geq 0$$
$$= 2[G(\eta-\eta_+) - G(\eta_c-\eta_+)] + \exp(\eta_2-\eta_+)[G(\eta_c-\eta_2) - G(\eta-\eta_2)] + \beta\delta[G(\eta^*-\eta_2^*) - G(\eta_c^*-\eta_2^*)] + \alpha\exp(\eta_+-\eta_c)\,G(\eta_c-\eta) + \gamma\delta\exp(\eta_2^*-\eta_c^*)\,\#(\eta_c^*-\eta^*),$$
$$\eta \geq \eta_+\,,\quad \eta' \leq 0$$
$$= 2[\exp(\eta-\eta_+) - 1 - G(\eta_c-\eta_+)] + \exp(\eta_2-\eta_+)[G(\eta_c-\eta_2) - G(\eta-\eta_2)] + \beta\delta[G(\eta^*-\eta_2^*) - G(\eta_c^*-\eta_2^*)] + \alpha\exp(\eta_+-\eta_c)\,G(\eta_c-\eta) + \gamma\delta\exp(\eta_2^*-\eta_c^*)\,\#(\eta_c^*-\eta^*),$$
$$\eta \leq \eta_+\,,\quad \eta' < 0\,.$$

Case 2(c)

$$\vec{n}_-(\eta) = \exp(\eta-\eta_+)[1 + E(\eta-\eta_c)], \qquad \eta' \leq 0$$
$$= \exp(\eta-\eta_+)[1 - E(\eta-\eta_c)], \qquad \eta' \geq 0$$
$$\overleftarrow{n}_-(\eta) = \exp(\eta^*-\eta_2^*)[1 + E(\eta^*-\eta_c^*)], \qquad \eta' \geq 0$$
$$= \exp(\eta^*-\eta_2^*)[1 - E(\eta^*-\eta_c^*)], \qquad \eta' \leq 0$$
$$\vec{n}_+(\eta) = \exp(\eta_+-\eta)[1 - 2E(\eta_+-\eta) + E(\eta_2-\eta)], \qquad \eta \leq \eta_+$$
$$= \exp(\eta_+-\eta)[1 + E(\eta_2-\eta)], \qquad \eta \geq \eta_+$$
$$\overleftarrow{n}_+(\eta) = \exp(\eta_2^*-\eta^*)[1 - E(\eta_2^*-\eta^*)],$$
$$F(\eta) = \exp(\eta_c-\eta_+)\,\#(\eta-\eta_c) + \beta\delta\exp(\eta_c^*-\eta_2^*)\,G(\eta^*-\eta_c^*) + \alpha\{\exp(\eta_+-\eta_2)[G(\eta_2-\eta_c) - G(\eta_2-\eta)] + 2[G(\eta_+-\eta) - G(\eta_+-\eta_c)]\} + \gamma\delta[G(\eta_2^*-\eta^*) - G(\eta_2^*-\eta_c^*)]$$
$$\eta \leq \eta_+\,,\quad \eta' \leq 0$$
$$= \exp(\eta_c-\eta_+)\,G(\eta-\eta_c) + \beta\delta\exp(\eta_c^*-\eta_2^*)\,\#(\eta^*-\eta_c^*) + \alpha\{\exp(\eta_+-\eta_2)[G(\eta_2-\eta_c) - G(\eta_2-\eta)] + 2[G(\eta_+-\eta) - G(\eta_+-\eta_c)]\} + \gamma\delta[G(\eta_2^*-\eta^*) - G(\eta_2^*-\eta_c^*)],$$
$$\eta \leq \eta_+\,,\quad \eta' \geq 0$$
$$= \exp(\eta_c-\eta_+)\,G(\eta-\eta_c) + \beta\delta\exp(\eta_c^*-\eta_2^*)\,\#(\eta^*-\eta_c^*) + \alpha\{\exp(\eta_+-\eta_2)[G(\eta_2-\eta_c) - G(\eta_2-\eta)] + 2[\exp(\eta_+-\eta) - 1 - G(\eta_+-\eta_c)]\} + \gamma\delta[G(\eta_2^*-\eta^*) - G(\eta_2^*-\eta_c^*)],$$
$$\eta \geq \eta_+\,,\quad \eta' > 0\,.$$

If the preceding expressions are restricted to the case of equal temperatures of both end plates, i.e. $T = T^*$, it results

$$\delta = 1;\ \beta = 1:$$
$$\gamma = \alpha\exp(-2\eta_d) \qquad [\text{see eq.(B4)}].$$

The above mentioned cases reduce now to three potential shapes as one can see from the following scheme.

cases 1(a), 2(a)[+] ⟶ case A
1(b), 1(c)[+] ⟶ B
2(c), 2(b)[+] ⟶ C

[+]The emitters I and II and also the parameters α and ν change their roles].

Type A

$$F'(\gamma) = \exp(\gamma-\gamma_d)\{1+\exp(2\gamma_d)+E(\gamma+\gamma_d)[1-\exp(2\gamma_d)]\} - 2\alpha\exp(-\gamma_d-\gamma), \tag{A1}$$

$$F(\gamma) = F(-\gamma_d) + G(\gamma+\gamma_d)[1-\exp(-2\gamma_d)] + 2[\exp(\gamma-\gamma_d) - \exp(-2\gamma_d)] + 2\alpha[\exp(-\gamma_d-\gamma)-1]; \tag{A2}$$

Type B ($\eta_e > +\eta_d$)

$\gamma \le \gamma_d$, $\gamma' > 0$:

$$F'(\gamma) = \exp(\gamma-\gamma_d)\{1+\exp(2\gamma_d) + E(\gamma+\gamma_d)[1-\exp(2\gamma_d)]\} - 2\alpha\exp(-\gamma_d-\gamma), \tag{A3}$$

$$F(\gamma) = [G(\gamma+\gamma_d)-G(\gamma_e+\gamma_d)][1-\exp(-2\gamma_d)] + 2[\exp(\gamma-\gamma_d)-1-G(\gamma_e-\gamma_d)] + 2\alpha[\exp(-\gamma_d-\gamma)-\exp(-\gamma_d-\gamma_e)]; \tag{A4}$$

$\gamma \ge \gamma_d$, $\gamma' \ge 0$:

$$F'(\gamma) = \exp(\gamma-\gamma_d)\{1+\exp(2\gamma_d)+E(\gamma+\gamma_d)[1-\exp(2\gamma_d)] - 2E(\gamma-\gamma_d)\} - 2\alpha\exp(-\gamma_d-\gamma), \tag{A5}$$

$$F(\gamma) = [G(\gamma+\gamma_d)-G(\gamma_e+\gamma_d)][1-\exp(-2\gamma_d)] + 2[G(\gamma-\gamma_d)-G(\gamma_e-\gamma_d)] + 2\alpha[\exp(-\gamma_d-\gamma)-\exp(-\gamma_d-\gamma_e)]; \tag{A6}$$

$\gamma \ge \gamma_d$, $\gamma' \le 0$:

In this case the formulae are identical with eqs. (A5) and (A6).

Type C ($\eta_e < -\eta_d$)

$\gamma \le -\gamma_d$, $\gamma' \le 0$:

$$F'(\gamma) = \exp(\gamma-\gamma_d)\{1+\exp(2\gamma_d)-E(\gamma-\gamma_e)[1-\exp(2\gamma_d)]\} - 2\alpha\exp(-\gamma_d-\gamma)[1-E(-\gamma_d-\gamma)], \tag{A7}$$

$$F(\gamma) = \exp(\gamma_e-\gamma_d)\,G(\gamma-\gamma_e)[1-\exp(2\gamma_d)] + 2[\exp(\gamma+\gamma_d)-\exp(\gamma_e+\gamma_d)] + 2\alpha[G(-\gamma_d-\gamma)-G(-\gamma_d-\gamma_e)]; \tag{A8}$$

$\gamma \le -\gamma_d$, $\gamma' \ge 0$:

$$F'(\gamma) = \exp(\gamma-\gamma_d)\{1+\exp(2\gamma_d)+E(\gamma-\gamma_e)[1-\exp(2\gamma_d)]\} - 2\alpha\exp(-\gamma_d-\gamma)[1-E(-\gamma_d-\gamma)], \tag{A9}$$

$$F(\gamma) = -\exp(\gamma_e-\gamma_d)\,G(\gamma-\gamma_e)[1-\exp(2\gamma_d)] + 2[\exp(\gamma-\gamma_d)-\exp(\gamma_e-\gamma_d)] + 2\alpha[G(-\gamma_d-\gamma)-G(-\gamma_d-\gamma_e)]; \tag{A10}$$

$\gamma \ge -\gamma_d$, $\gamma' > 0$:

$$F'(\gamma) = \exp(\gamma-\gamma_d)\{1+\exp(2\gamma_d)+E(\gamma-\gamma_e)[1-\exp(2\gamma_d)]\} - 2\alpha\exp(-\gamma_d-\gamma), \tag{A11}$$

$$F(\gamma) = -\exp(\gamma_e-\gamma_d)\,G(\gamma-\gamma_e)[1-\exp(2\gamma_d)] + 2[\exp(\gamma-\gamma_d)-\exp(\gamma_e-\gamma_d)] + 2\alpha[\exp(-\gamma_d-\gamma)-1-G(-\gamma_d-\gamma_e)]; \tag{A12}$$

Equations (A1)...(A12) are the equations we started from in the body of the paper.

APPENDIX B

Calculation of the parameter ν:

The process of ionization at the surface of a hot end plate is, to a high degree of accuracy, described by the LANGMUIR-SAHA equation /12/

$$\frac{\nu_+}{\nu_o} = \frac{\text{ion evaporation rate}}{\text{neutral evaporation rate}} = \frac{g_+}{g_o} \exp\left\{e\,\frac{(\Phi_+ - I)}{kT}\right\}.$$

The probability P for a particle, ion or neutral, to be ionized after hitting the emitter plate is equal for both kinds of incoming particles and is given by

$$P = \left(1 + \frac{\nu_o}{\nu_+}\right)^{-1}.$$

It has been shown experimentally by ZANDBERG and TONTEGODE /7/ that the ionization probability P is nearly unity for cesium at polycrystalline refractory metals. For sake of simplicity we use for the present calculations

$$P = 1. \tag{B1}$$

1) Potential shapes of type A and C respectively.

$$j_{+\rightarrow} = P(j_{o\leftarrow} + j_{+\leftarrow}) + P\sum_1 P^\nu (j_{o\leftarrow} + j_{+\leftarrow})(1 - \exp(-2\eta_d))^\nu,$$

$$= P\sum_o P^\nu (j_{o\leftarrow} + j_{+\leftarrow})(1 - \exp(-2\eta_d))^\nu$$

$$= \frac{P(j_{o\leftarrow} + j_{+\leftarrow})}{1 - P(1 - \exp(-2\eta_d))^\nu};$$

$$j_{+\leftarrow} = P\left[j_{o\leftarrow} + j_{+\rightarrow}\exp(-2\eta_d)\right];$$

$$j_{o\rightarrow} + j_{+\rightarrow}\exp(-2\eta_d) = j_{o\leftarrow} + j_{+\leftarrow}.$$

Combining these equations results in the equation

$$j_{+\rightarrow} = j_{+\leftarrow}\left[1 - P\left[1 - \exp(-2\eta_d)\right]\right]^{-1}. \tag{B2}$$

Assuming P = 1 we arrive at the relation

$$j_{+\leftarrow} = j_{+\rightarrow}\exp(-2\eta_d),$$

which may be rewritten in the following form

$$\nu = \alpha\exp(-2\eta_d).$$

2) Potential shape type B.

In an analogous procedure we receive

$$j_{+\rightarrow} = P(j_{o\leftarrow} + j_{+\leftarrow}\exp(\eta_d - \eta_e)) + P\sum_1 P^\nu (j_{o\leftarrow} + j_{+\leftarrow}\exp(\eta_d - \eta_e))(1 - \exp(-\eta_d - \eta_e))^\nu$$

$$j_{+\leftarrow} = P\sum_o P^\nu (1 - \exp(\eta_d - \eta_e))^\nu (j_{o\rightarrow} + j_{+\rightarrow}\exp(-\eta_d - \eta_e));$$

$$j_{o\rightarrow} + j_{+\rightarrow}\exp(-\eta_d - \eta_e) = j_{o\leftarrow} + j_{+\leftarrow}\exp(\eta_d - \eta_e);$$

and

$$j_{+\leftarrow} = j_{+\rightarrow}\frac{1 - P(1 - \exp(-\eta_d - \eta_e))}{1 - P(1 - \exp(\eta_d - \eta_e))} \tag{B3}$$

If eq.(B1) holds, we get

$$j_{+\leftarrow} = j_{+\rightarrow} \exp(-2\eta_d),$$

or

$$\nu = \alpha \exp(-2\eta_d).$$

We summarize: With the assumptions used in this paper we get the relation

$$\nu = \alpha \exp(-2\eta_d) \qquad (B4)$$

for all types of potential shapes.

ACKNOWLEDGEMENT

It is a pleasure to acknowledge numerous illuminating conversations with Drs. E. Guilino and W. Ott in the course of this work. Their comments have been of considerable value in clarifying certain points. The author also wishes to thank P. Piotrowski for his help in programming the numerical calculations reported in this paper.

BIBLIOGRAPHY

/1/ P.L. AUER
H. HURWITZ
JAP 30, 161 (1959)

/2/ R.G. McINTYRE
JAP 33, 2485 (1962);
Advanced Energy Conversion 2, 405 (1962);
Proc. IEEE 51, 760 (1963)

/3/ A.L. EICHENBAUM
K.G. HERNQVIST
JAP 32, 16 (1961)

/4/ N. RYNN
Phys. Fluids 9, 165 (1966)

/5/ A. SESTERO
M. ZANNETTI
Nuovo Cim. 51, 230 (1967)

/6/ P.N. HU
S. ZIERING
Phys. Fluids 9, 2168 (1966)

/7/ E.Ya. ZANDBERG
A.Ya. TONTEGODE
Sov.Phys.-Techn.Phys. 10, 1162 (1966);
8th Int.Conf. Phen. in Ionized Gases,
Vienna, 1967, p. 69

/8/ J.B. TAYLOR
I. LANGMUIR
Phys.Rev. 44, 423 (1933)

/9/ M. TROPPMANN
Report IPP 2/79, July 1969,
to be published

/10/ R.Ya. KUCHEROV
L.E. RIKENGLAZ
Sov.Phys.-Techn.Phys. 7, 941 (1963)

/11/ P.L. AUER
JAP 31, 2096 (1960)

/12/ S. DATZ
E.H. TAYLOR
J.Chem.Phys. 25, 389 (1956)

FIGURE CAPTIONS

Fig. 1 The model used for calculations

Fig. 2 Trial distributions of potential between electrodes
a) Potential shape of type A
b) Potential shape of type B
c) Potential shape of type C

Fig. 3 Potential shape of type A and its limiting cases
a) Transition A to C
—.—. type A
——— $\eta'(\eta = -\eta_d) = 0$; $\eta''(\eta = -\eta_d) \neq 0$
---- type C

b) Transition A to B
---- type B
——— $\eta'(\eta = +\eta_d) = 0$; $\eta''(\eta = +\eta_d) = 0$
—.—. type A

c) Type A
---- $\eta''(\eta = -\eta_d) > 0$
——— $\eta''(\eta = -\eta_d) = 0$ } $\eta'(\eta = -\eta_d) \neq 0$
—.—. $\eta''(\eta = -\eta_d) < 0$ }

Fig. 4 Limiting case of potential shapes of type A(see fig. 3a); plasma potential vs. diode voltage

Fig. 5 Plasma potential vs. diode voltage for the potential shape of type A with vanishing space charge density near the emitter I at $-\eta_d$(see fig.3c)

Fig. 6 Regions of various potential distributions in parameter space. The broken line separates electron and ion sheath in front of the negative emitter

Fig. 7 The second deviation of the actual potential η as a function of η for the case of potential shape of type B (eqs. (A3), (A5)); $\alpha = 2$

Fig. 8 Potential distribution of type B; values of plasma potential and potential extrema for given values of η_d

Fig. 9 Potential shape of type C
a) Cross-section of the solution surface for $\alpha = 0.2$
b) Contour lines of the space charge and electric field equations respectively
$F \hat{=} \eta'$; $F' \hat{=} \eta''$
——— I (fig. 2(c2))
—..—.. II (fig. 2(c3))
---- III (fig. 2(c4))

Fig. 10 Potential distributions of type C with monotonic varying sheaths (fig. 2(c1))

Fig. 11 Cut surface of the two equations $F' = 0$ and $F = 0$ (equations of the space charge density and of the electric field at the plasma boundary)
a) ion-rich emission, $\alpha > 1$
b) electron-rich emission $\alpha < 1$, $\eta_p = \eta_e$
c) electron-rich emission $\alpha < 1$, $\eta_p \neq \eta_e$

Fig. 12 a) Cross-section of the solution surface (fig. 11) parallel to the axis of the parameter α; $\eta_d = 1.2$
b) Potential distributions for various values of α (schematically)

Fig. 13 a) Cross-section parallel to the axis of the diode voltage η_d: $\alpha = 0.65$
b) Schematic potential shapes for different values of η_d

Fig. 14 see fig. 13; $\alpha = 10$

Fig. 15 Shapes of potential distributions

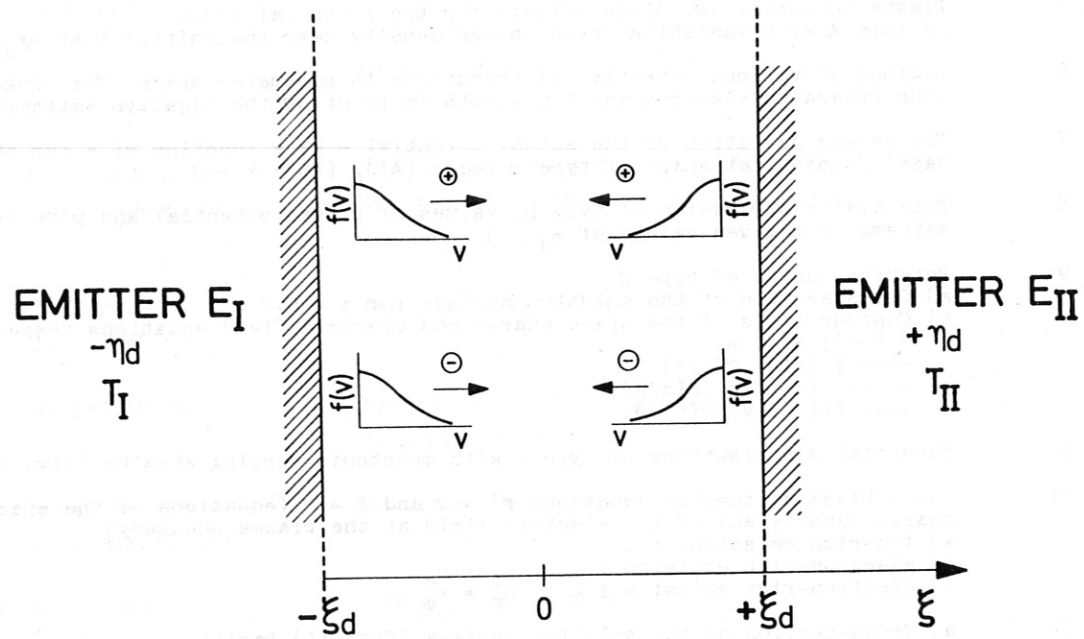

Fig. 1

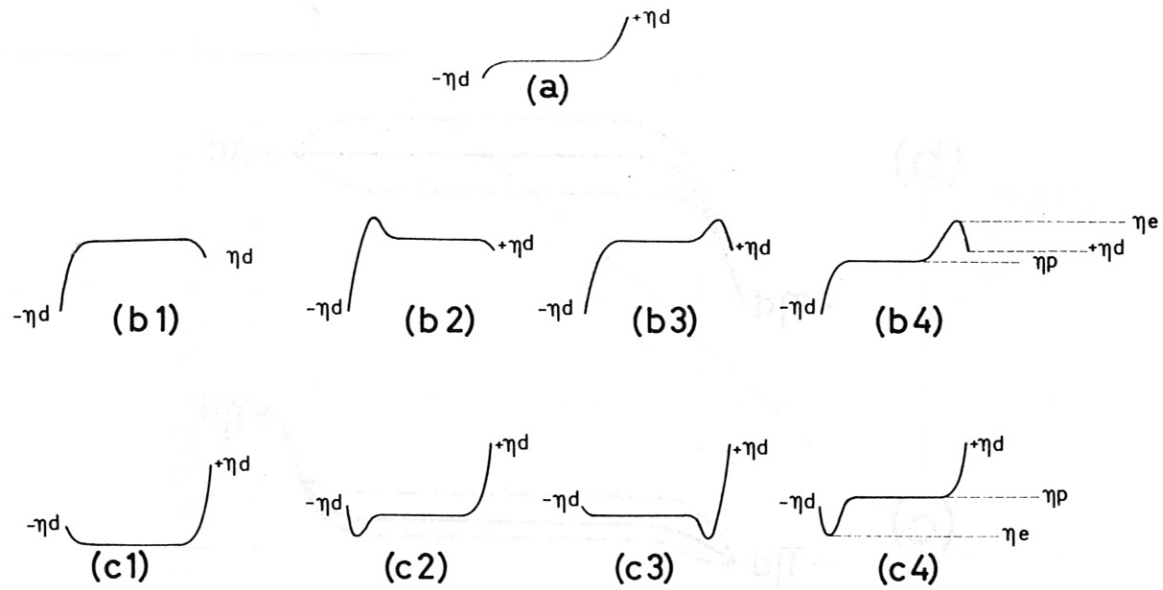
-ηd
+ηd
(a)
-ηd
ηd
(b 1)
-ηd
+ηd
(b 2)
-ηd
+ηd
(b3)
-ηd
ηe
+ηd
ηp
(b4)
-ηd
+ηd
(c1)
-ηd
+ηd
(c2)
-ηd
+ηd
(c3)
-ηd
+ηd
ηp
ηe
(c4)

Fig. 2

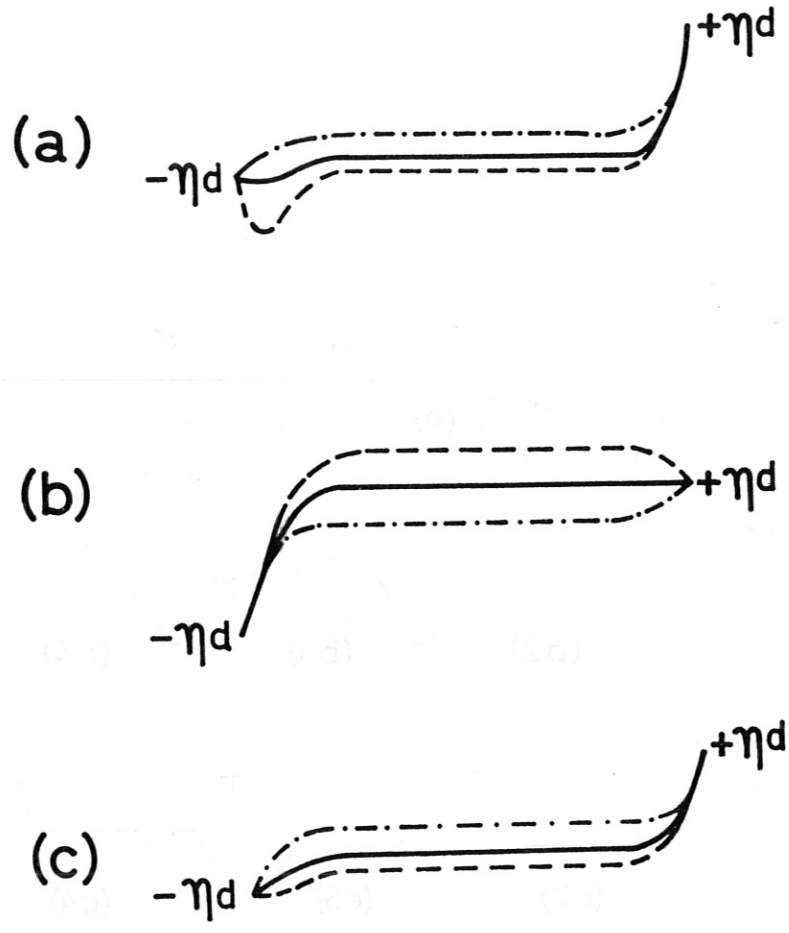

Fig. 3

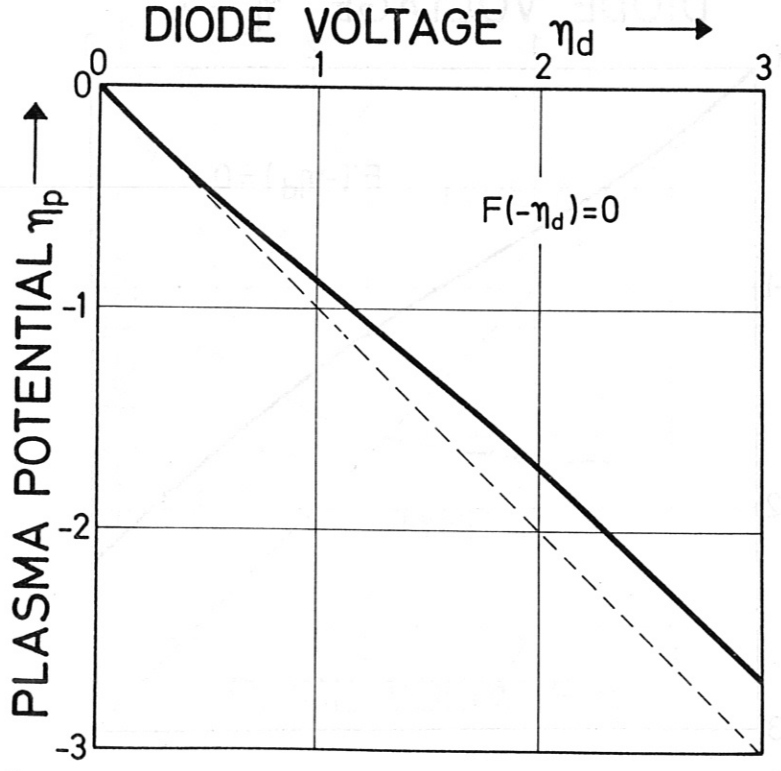

Fig. 4

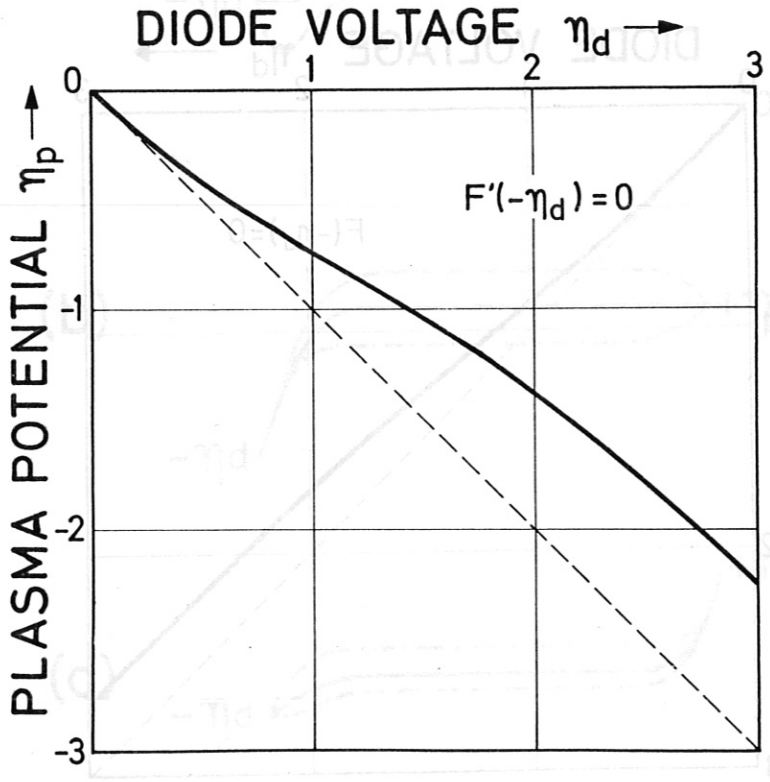

Fig. 5

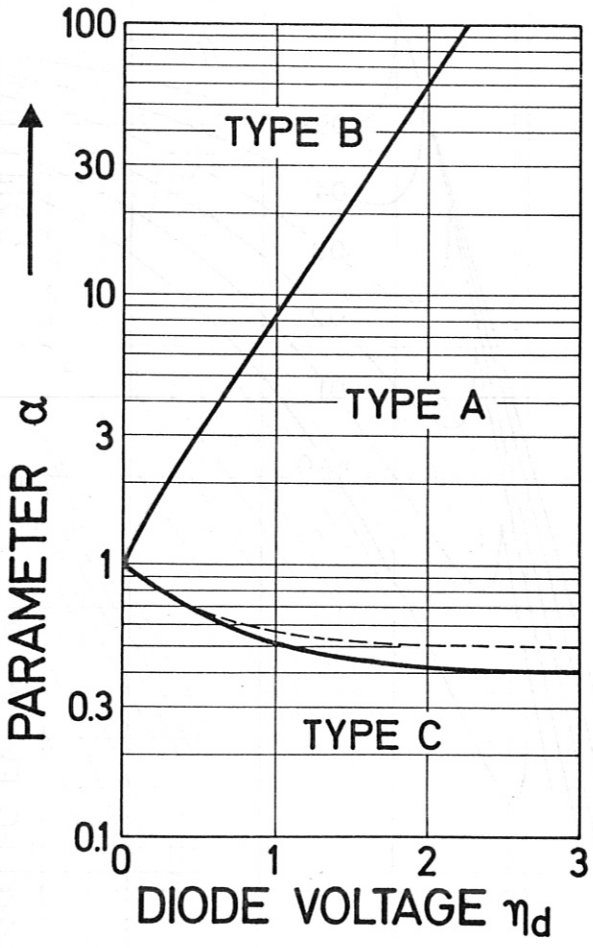
100
30
10
3
1
0.3
0.1
PARAMETER α
TYPE B
TYPE A
TYPE C
0
1
2
3
DIODE VOLTAGE η_d

Fig. 6

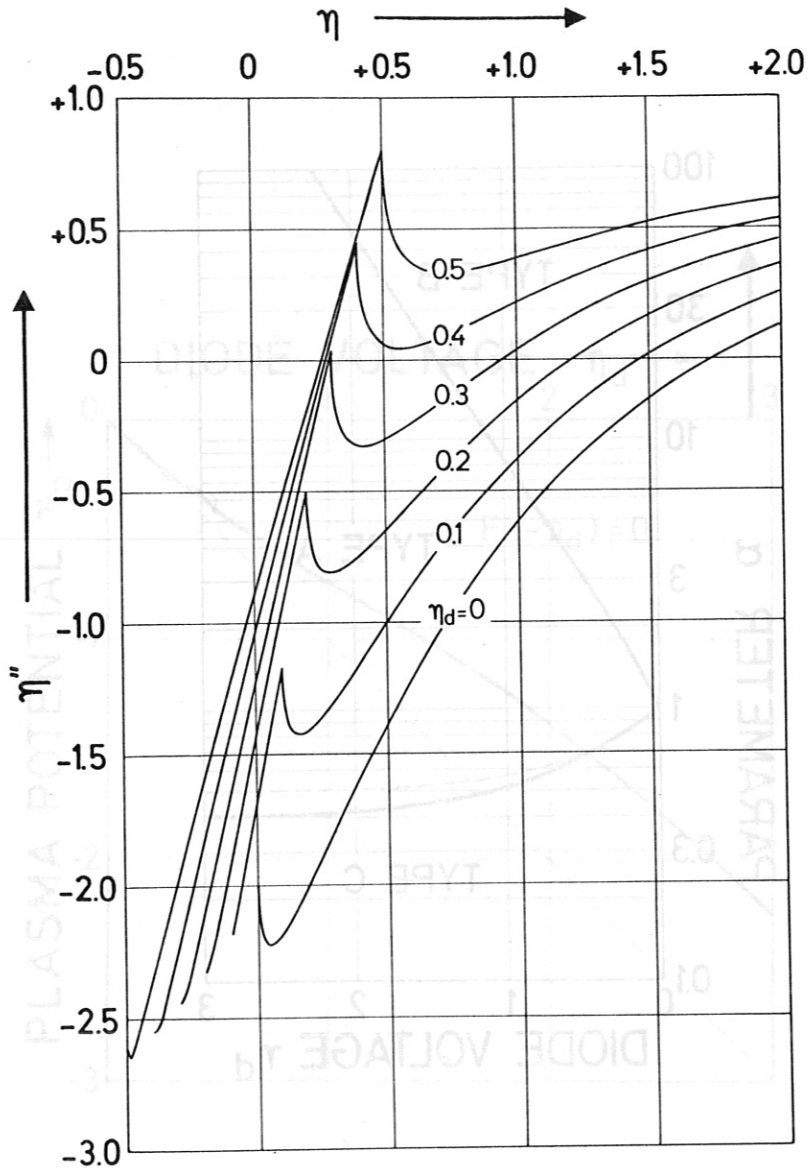

Fig. 7

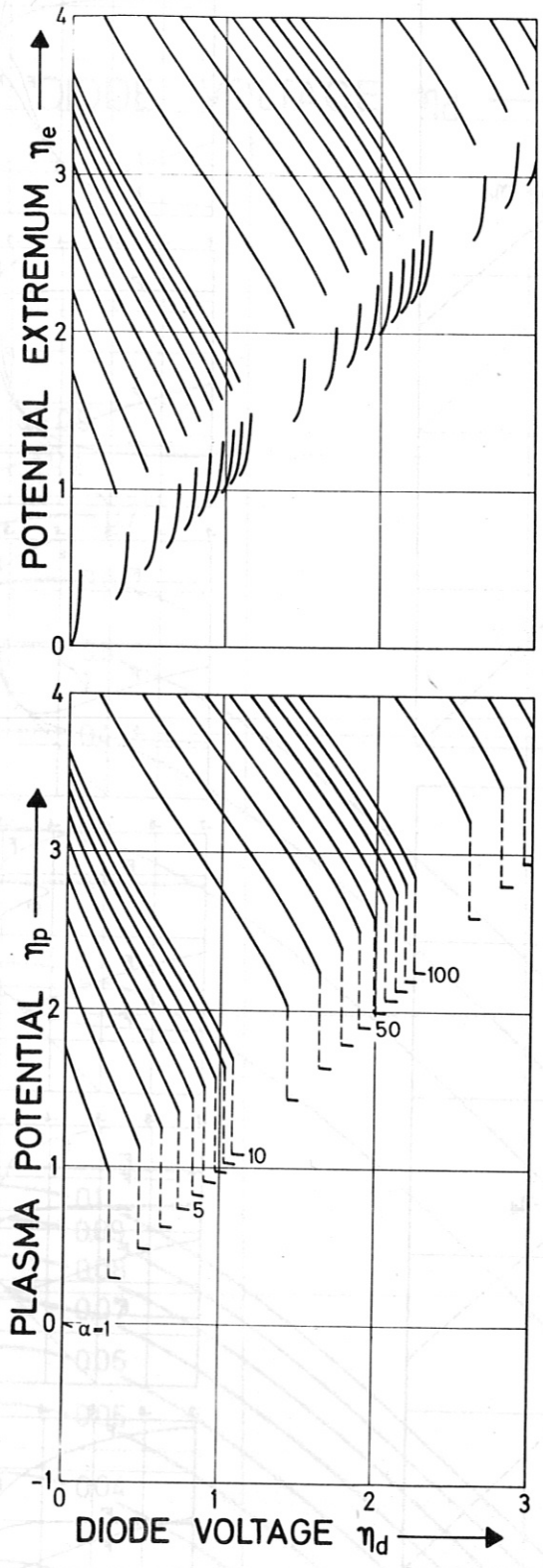
POTENTIAL EXTREMUM η_e
PLASMA POTENTIAL η_p
DIODE VOLTAGE η_d
α=1
5
10
50
100
0
1
2
3
4
-1

Fig. 8

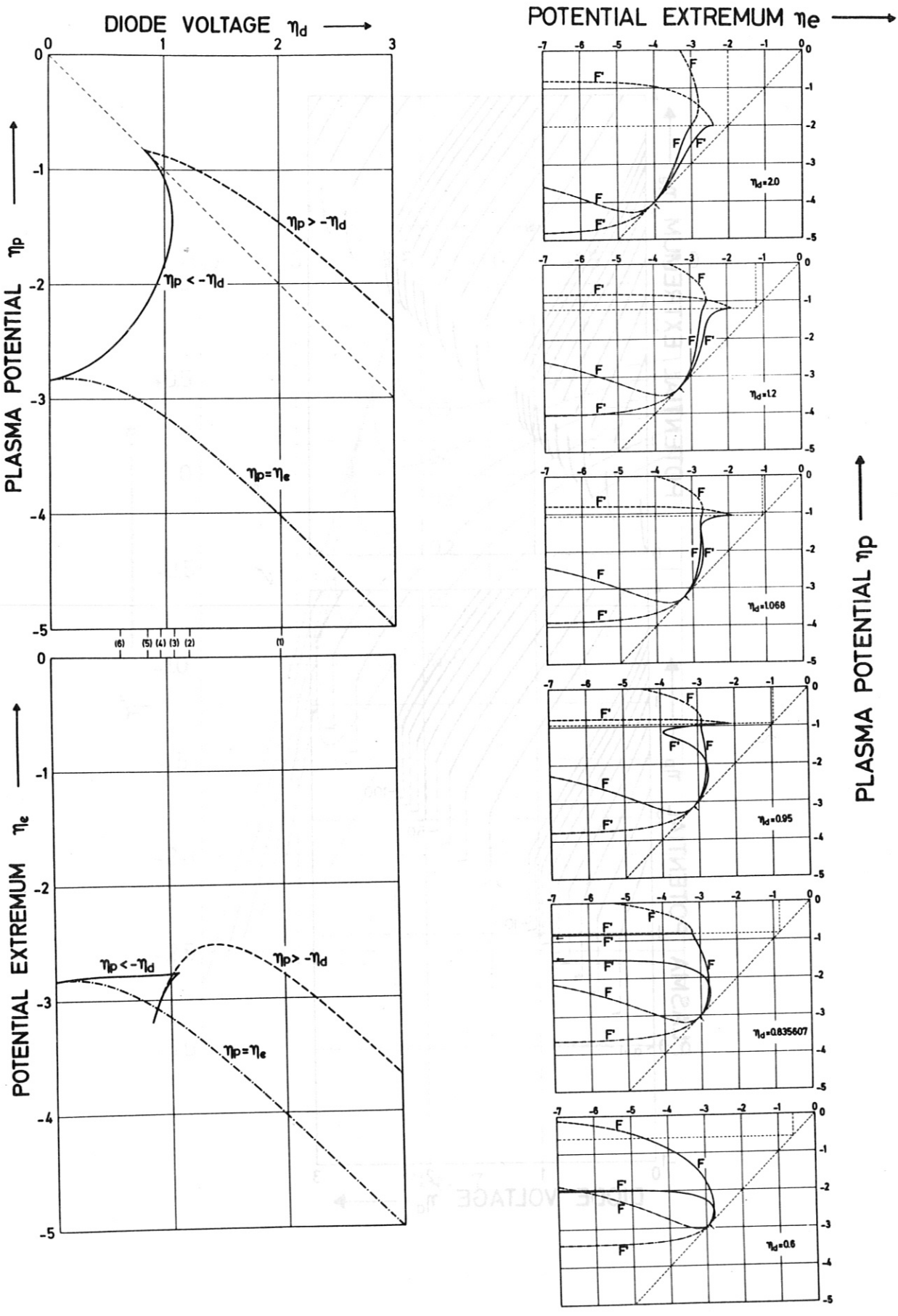
DIODE VOLTAGE η_d
PLASMA POTENTIAL η_p
$\eta_p > -\eta_d$
$\eta_p < -\eta_d$
$\eta_p = \eta_e$
(6) (5) (4) (3) (2) (1)
POTENTIAL EXTREMUM η_e
$\eta_p < -\eta_d$
$\eta_p > -\eta_d$
$\eta_p = \eta_e$
(a)
POTENTIAL EXTREMUM η_e
PLASMA POTENTIAL η_p
F
F'
η_d=2.0
η_d=1.2
η_d=1.068
η_d=0.95
η_d=0.835607
η_d=0.6
(b)

Fig. 9

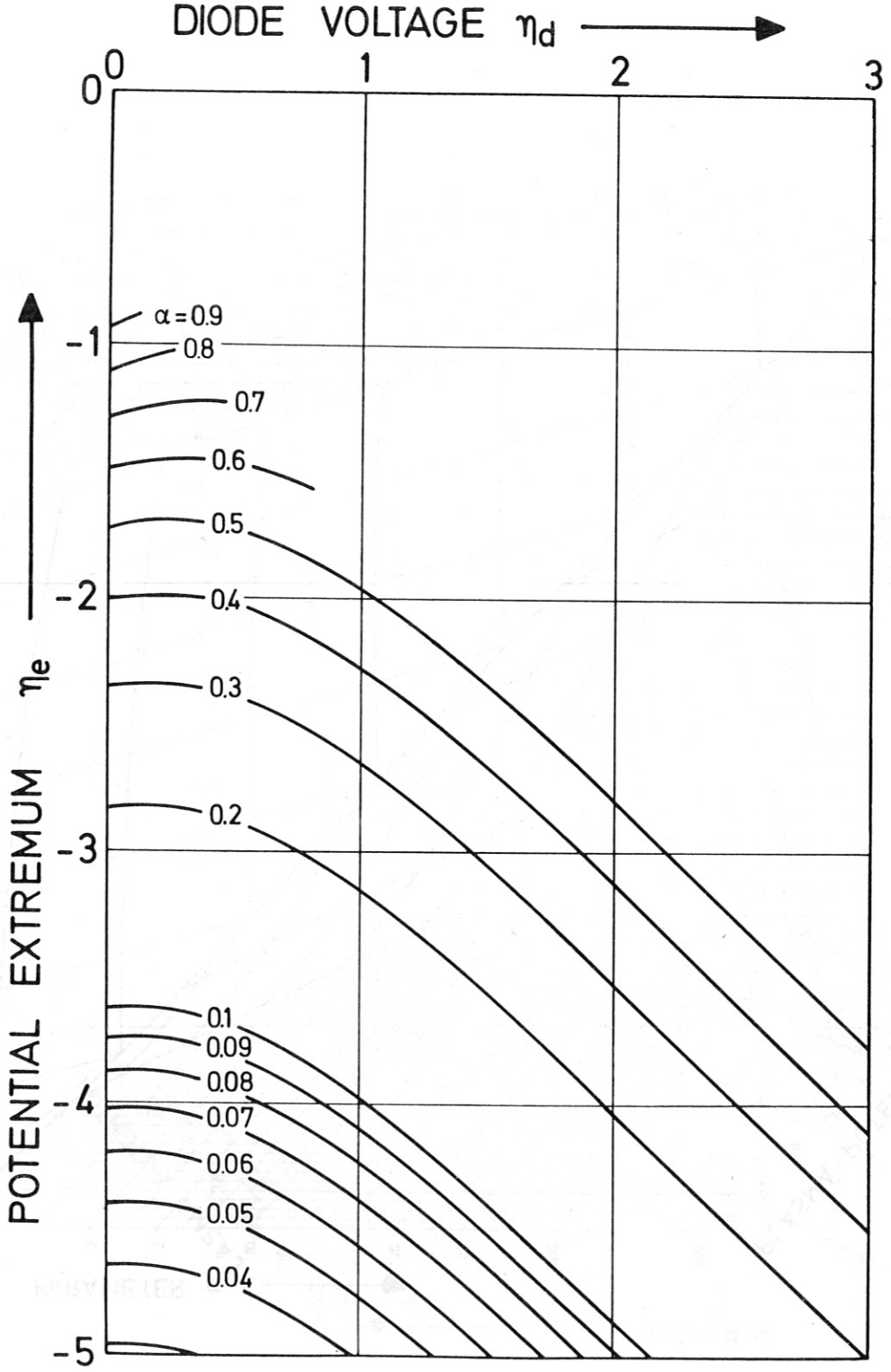
DIODE VOLTAGE η_d
0
1
2
3
POTENTIAL EXTREMUM η_e
-1
-2
-3
-4
-5
α = 0.9
0.8
0.7
0.6
0.5
0.4
0.3
0.2
0.1
0.09
0.08
0.07
0.06
0.05
0.04

Fig. 10

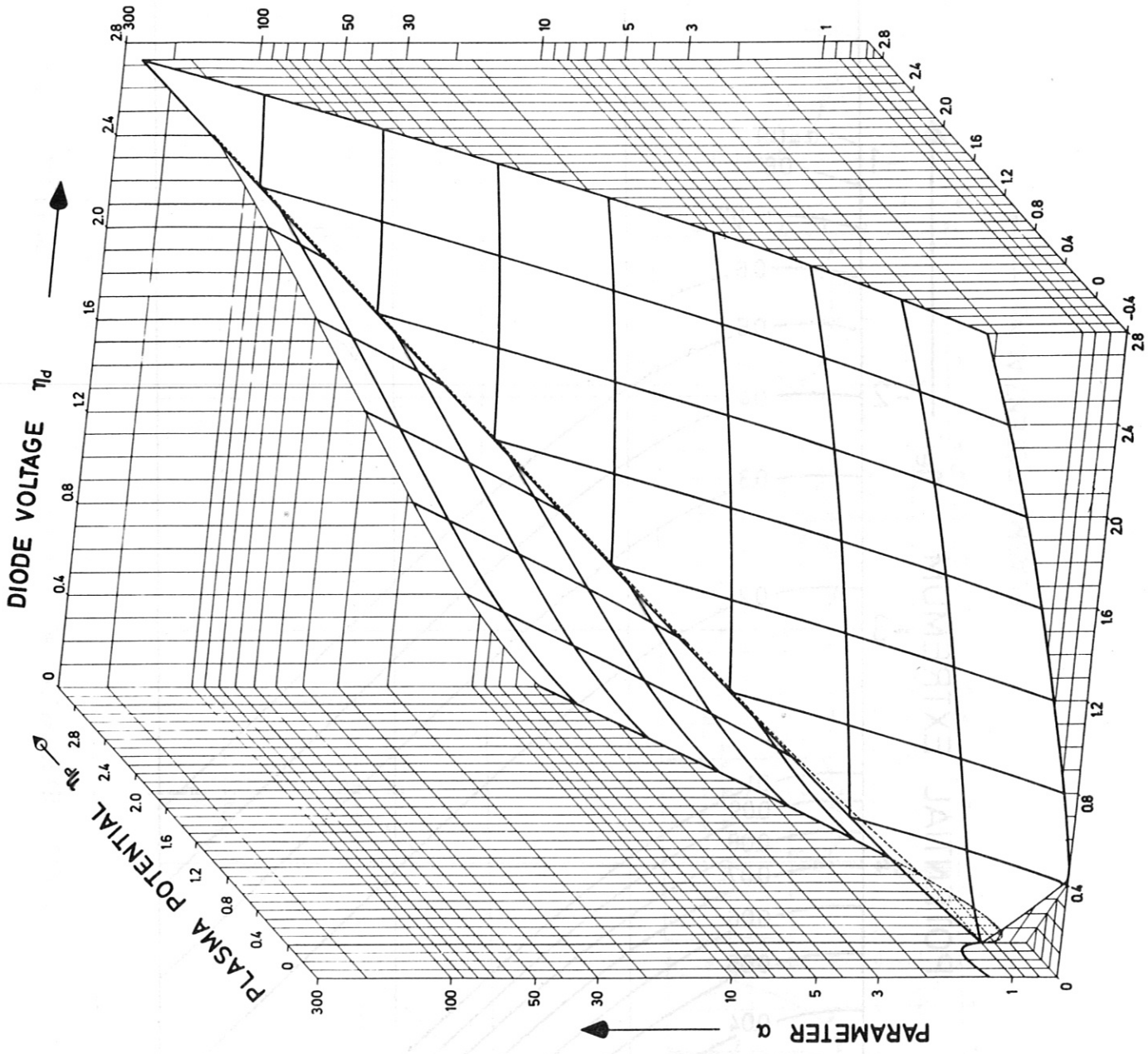
DIODE VOLTAGE η_d
PLASMA POTENTIAL Φ
PARAMETER α
0
0.4
0.8
1.2
1.6
2.0
2.4
2.8
-0.4
300
100
50
30
10
5
3
1

Fig. 11 a

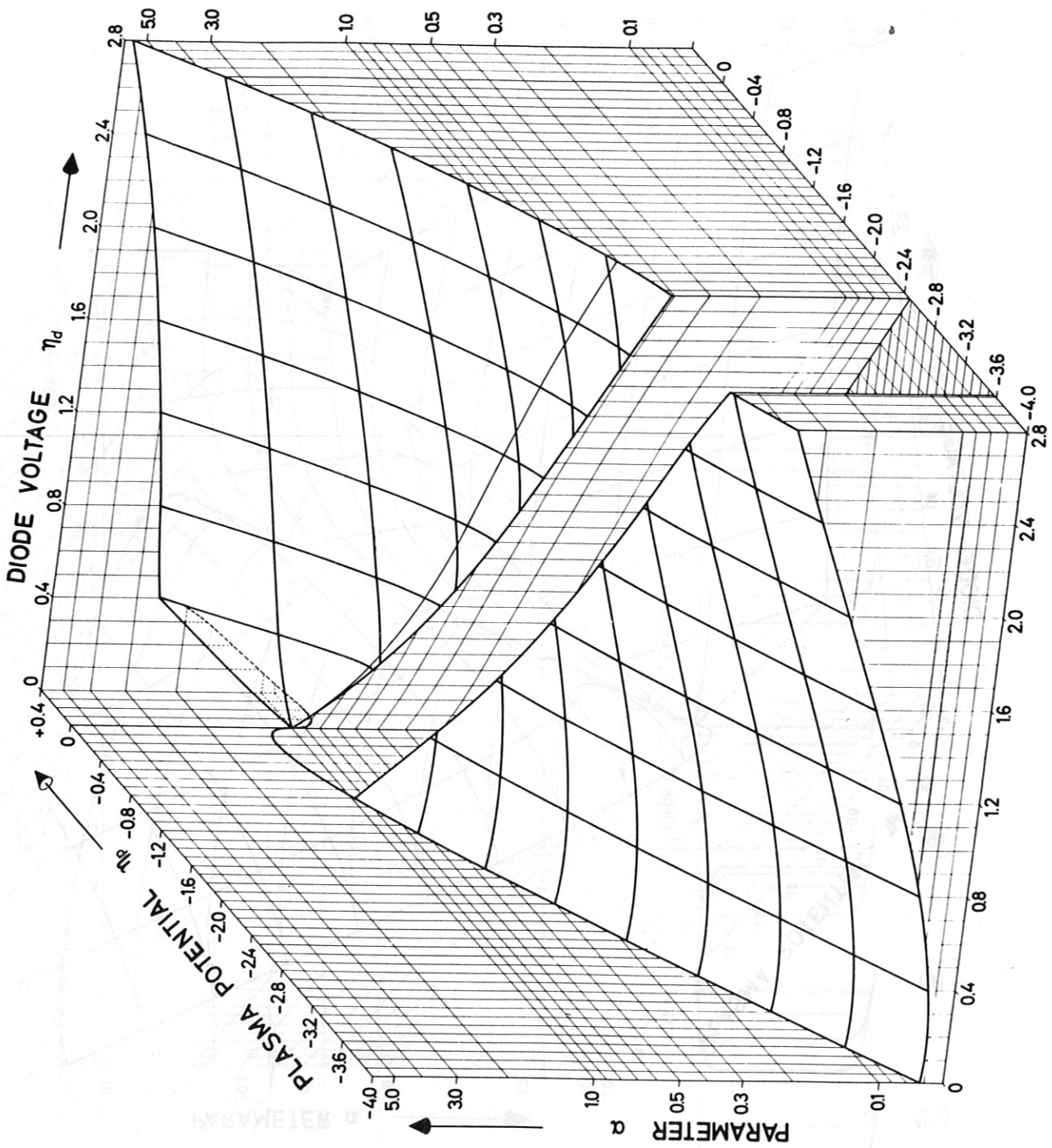
DIODE VOLTAGE η_d
PLASMA POTENTIAL $\hat{\eta}$
PARAMETER α
0
+0.4
0.4
0.8
1.2
1.6
2.0
2.4
2.8
-0.4
-0.8
-1.2
-1.6
-2.0
-2.4
-2.8
-3.2
-3.6
-4.0
5.0
3.0
1.0
0.5
0.3
0.1

Fig. 11 b

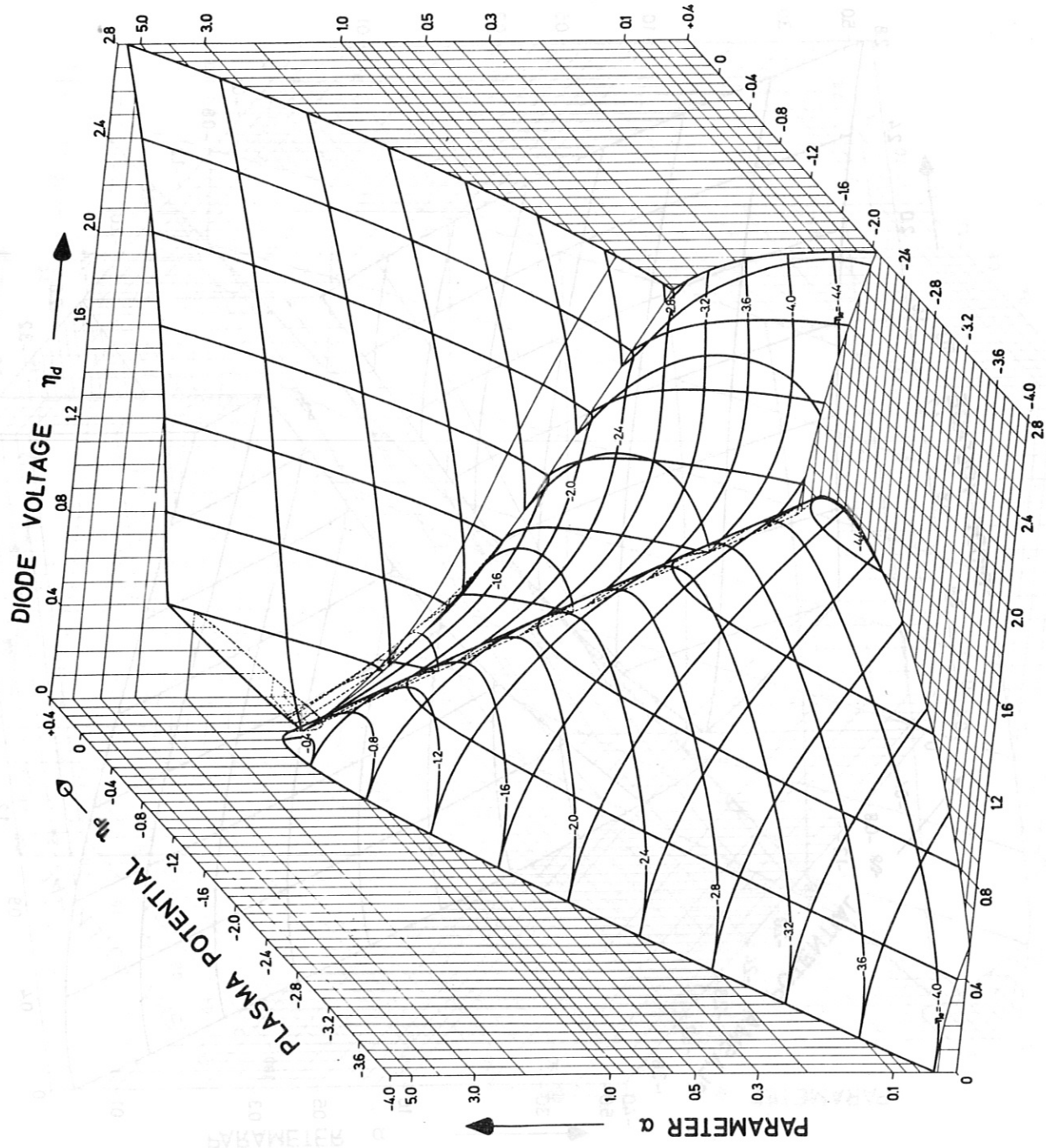

Fig. 11 c

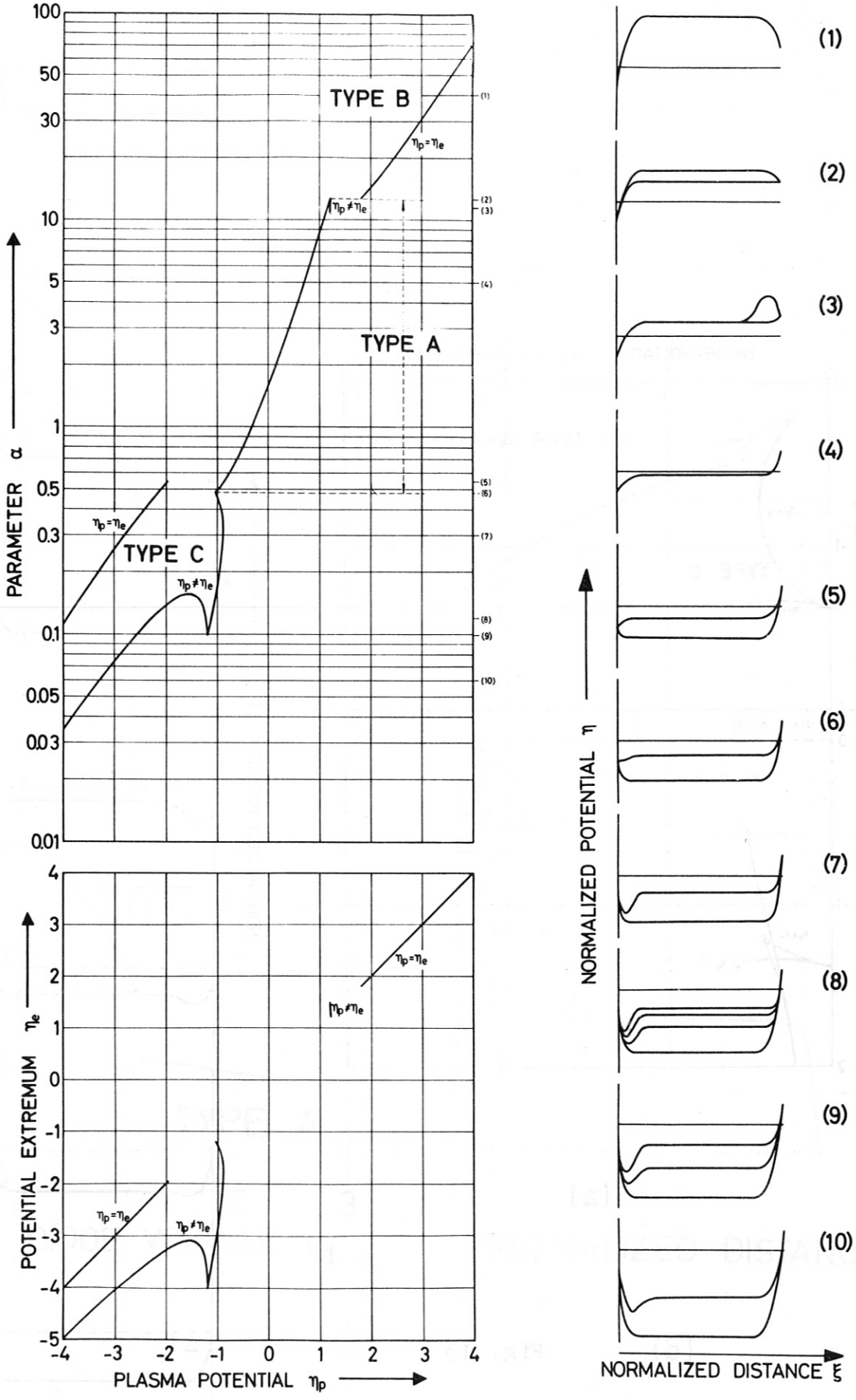
PARAMETER α
100
50
30
10
5
3
1
0.5
0.3
0.1
0.05
0.03
0.01
TYPE B
TYPE A
TYPE C
$\eta_p = \eta_e$
$\eta_p \neq \eta_e$
(1)
(2)
(3)
(4)
(5)
(6)
(7)
(8)
(9)
(10)
POTENTIAL EXTREMUM η_e
PLASMA POTENTIAL η_p
NORMALIZED POTENTIAL η
NORMALIZED DISTANCE ξ
(a)
(b)

Fig. 12

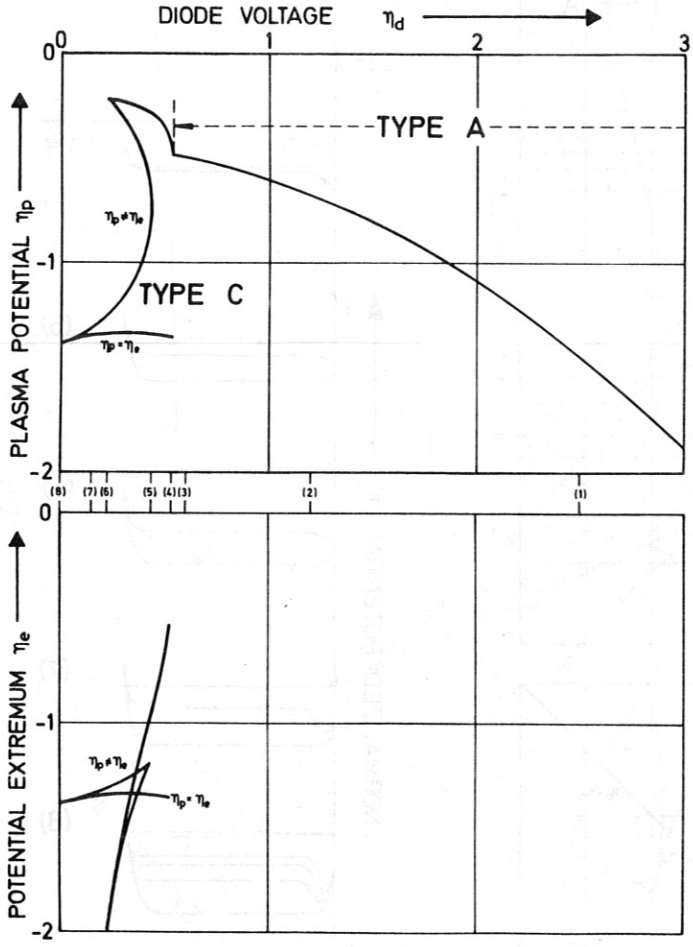
DIODE VOLTAGE η_d
0
1
2
3
TYPE A
TYPE C
$\eta_p \neq \eta_e$
$\eta_p = \eta_e$
PLASMA POTENTIAL η_p
0
-1
-2
(8) (7) (6) (5) (4) (3) (2) (1)
POTENTIAL EXTREMUM η_e
0
-1
-2
$\eta_p \neq \eta_e$
$\eta_p = \eta_e$

(a)

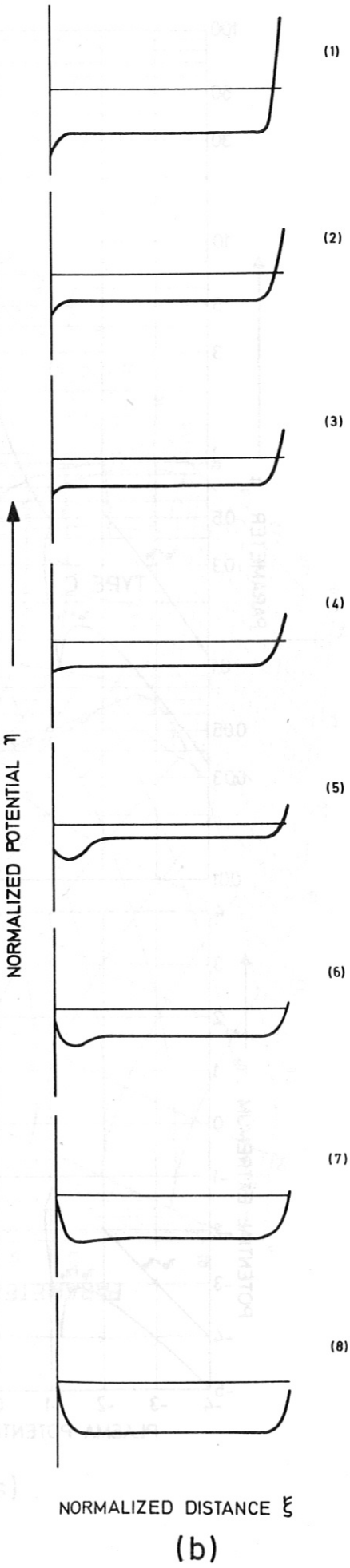
NORMALIZED POTENTIAL η
(1)
(2)
(3)
(4)
(5)
(6)
(7)
(8)
NORMALIZED DISTANCE ξ

(b)

Fig. 13

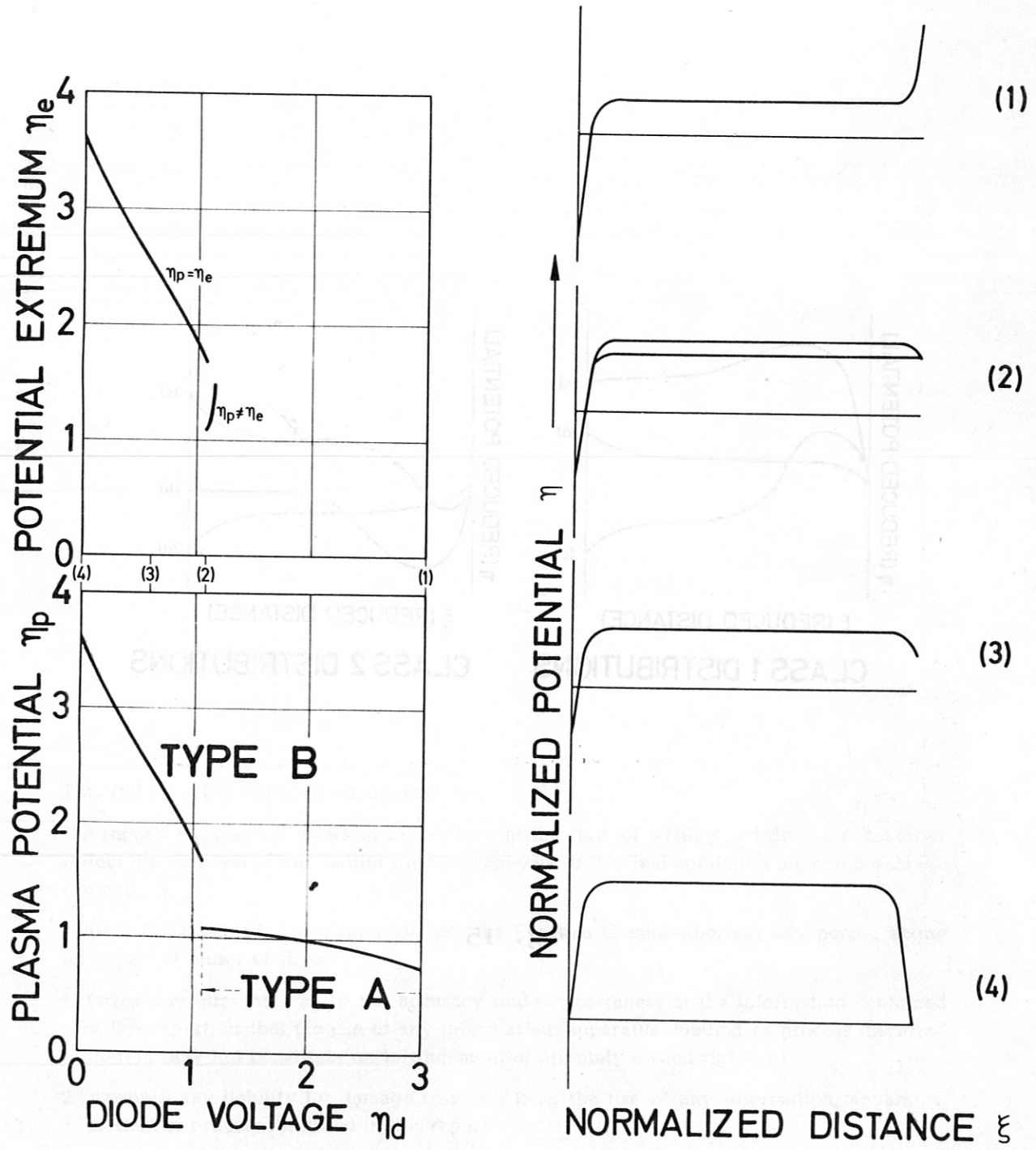
PLASMA POTENTIAL η_p
POTENTIAL EXTREMUM η_e
$\eta_p = \eta_e$
$\eta_p \neq \eta_e$
TYPE B
TYPE A
(4)
(3)
(2)
(1)
DIODE VOLTAGE η_d
(a)
NORMALIZED POTENTIAL η
NORMALIZED DISTANCE ξ
(1)
(2)
(3)
(4)
(b)

Fig. 14

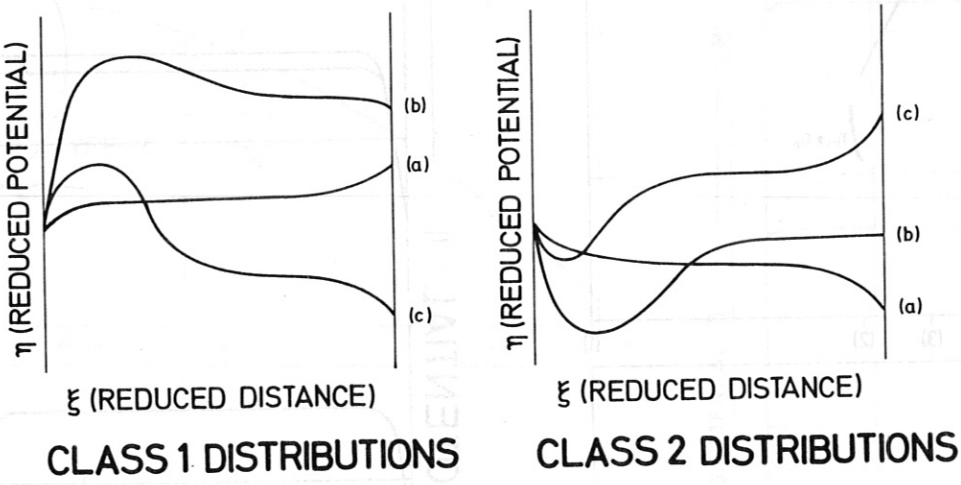
η (REDUCED POTENTIAL)
(b)
(a)
(c)
ξ (REDUCED DISTANCE)
CLASS 1 DISTRIBUTIONS
η (REDUCED POTENTIAL)
(c)
(b)
(a)
ξ (REDUCED DISTANCE)
CLASS 2 DISTRIBUTIONS

Fig. 15